R. & M. No. 3456

MINISTRY OF AVIATION

AERONAUTICAL RESEARCH COUNCIL
REPORTS AND MEMORANDA

The Unsteady Forces on Finite Wings in Transient Motion

By B. D. Dore, M.A., D.Phil.

Part I.—Initial Aerodynamic Forces Following a Sudden Change of Incidence

Part II.—Transient Lift and Moment Functions for Rectangular and Delta Wings

LONDON: HER MAJESTY'S STATIONERY OFFICE
1966

PRICE £1 0*s.* 0*d.* NET.

The Unsteady Forces on Finite Wings in Transient Motion

By B. D. Dore, M.A., D.Phil.

(Approved on behalf of Director, N.P.L. by Dr. R. C. Pankhurst, Superintendent of Aerodynamics Division.)

Reports and Memoranda No. 3456†
September, 1964

Part 1.—Initial Aerodynamic Forces Following a Sudden Change of Incidence*

Summary.
The forces and moments on wings of finite aspect ratio undergoing a sudden change of incidence are considered at the start of the unsteady motion. Linearized theory is used and the flow is assumed to be incompressible. The method adopted is only a slight extension of that suggested by R. T. Jones. Applications are made to rectangular and delta wings, but the method is suitable for many planforms. Spanwise and chordwise load distributions are given, and the position of the centre of lift is determined exactly in the case of a square wing. A comparison of the initial and final aerodynamic forces is made.

LIST OF CONTENTS

Section
1. Introduction
2. Analogy with Steady Flow
3. Exact Application of Analogy
   - 3.1. Initial forces and moments
   - 3.2. Particular results
4. Approximate Equations for Steady Flow without Circulation
   - 4.1. Wings of high aspect ratio
   - 4.2. Wings of low aspect ratio
5. Method of Solution for Wings of High Aspect Ratio
6. Method of Solution for Wings of Low Aspect Ratio
7. Impulsive Load Distribution
8. Initial Load Distribution
   - 8.1. Spanwise and chordwise loadings
   - 8.2. Special results for rectangular wings
   - 8.3. Special results for delta wings

†Part I replaces N.P.L. Aero Report 1113–A.R.C. 26 116
Part II replaces N.P.L. Aero Report 1115–A.R.C. 26 195

*The contents of this paper are drawn partly from the author's D.Phil. Thesis at the University of Oxford (May, 1963), and partly from work carried out subsequently at the National Physical Laboratory.

9. Numerical Results
9.1. Accuracy of results
9.2. Initial forces and moments
10. Comparisons between Initial and Final Values
11. Acknowledgements
List of Symbols
References
Appendix
Tables 1 to 7
Illustrations

1. *Introduction.*

The determination of the aerodynamic forces on a two-dimensional wing undergoing a sudden change of incidence has been considered by several writers. Von Kármán and Sears[1], Söhngen[2], Sears[3], Leehey[4] have made positive contributions to the original theory of Wagner[5], so that accurate assessments of the forces can be made.

However, for wings of finite span, the linearized theory for incompressible flow has been formulated but numerical applications are few. An approximate method was given by R. T. Jones[6], who calculated the growth of lift on elliptic wings of high aspect ratio. More recently, Vogel[7] has used an extension of lifting-line theory to calculate the spanwise distribution of lift as a function of time t. His method has so far been developed for wings with straight quarter-chord lines, but it appears to be somewhat inaccurate for small time. W. P. Jones[8] and Drischler[9] have used oscillatory lift coefficients to obtain the growth of lift function from the reciprocal relations of Garrick[10]. The method given by W. P. Jones is valid only for certain wings of high aspect ratio. That given by Drischler, who also calculates some spanwise distributions of lift, is unsuitable for a finite interval of time following the sudden change of incidence.

In Part I of this report, attention is concentrated on the forces and moments at the start of the unsteady motion. It is necessary to distinguish between those acting at $t = 0$ which are of an impulsive nature, and those acting at $t = 0+$ which are finite (*see* Sections 3, 7 and 8). The former will be qualified by 'impulsive' and the latter by 'initial' throughout the text. The method adopted to study the initial forces and moments is but a slight extension of that given by R. T. Jones. It has been applied to rectangular and delta wings for a fairly wide range of aspect ratio. The total initial lift on rectangular and delta wings has been calculated approximately by Lehrian[11] and Duquenne[12], the latter using directly the method suggested by R. T. Jones. Their results are compared with those of the present method in Sections 9 and 10.

The main objectives of Part I have been twofold. Firstly, to give initial spanwise and chordwise distributions of lift, since there appears to be no information on these quantities in the literature. Secondly, to investigate effects of aspect ratio and planform on the total initial lift. In Part II, it is shown how the calculated results of Part I may be applied to yield comparatively accurate assessments of the unsteady forces on finite wings in sudden plunging motion or entering a sharp-edged gust.

2. *Analogy with Steady Flow.*

Consider the translational motion of a flat wing moving with uniform velocity U in an incompressible, inviscid fluid and suppose that the angle of incidence is given as a function of time by

$$\alpha(t) = \alpha 1(t), \tag{1}$$

where the unit step-function

$$\left.\begin{aligned} 1(t) &= 0 \quad (t<0) \\ 1(t) &= 1 \quad (t\geqslant 0) \end{aligned}\right\}. \tag{2}$$

Thus, at $t = 0$, the incidence is suddenly changed from zero to a constant α. It is assumed that α is small and that the equations of linearized theory hold. Then, in the notation of Fig. 1a, the perturbation velocity potential $\phi(x,y,z,t)$ satisfies Laplace's equation

$$\frac{\partial^2\phi}{\partial x^2}+\frac{\partial^2\phi}{\partial y^2}+\frac{\partial^2\phi}{\partial z^2}=0, \tag{3}$$

together with the following conditions:

(a) for points (x,y,o) inside S,

$$\frac{\partial\phi}{\partial z}=-U\alpha 1(t); \tag{4}$$

(b) for points (x,y,o) inside W,

$$\frac{\partial\phi}{\partial t}+U\frac{\partial\phi}{\partial x}=0; \tag{5}$$

(c) for points (x,y,o) inside R,

$$\phi=0; \tag{6}$$

(d) if $t<0$,

$$\phi\equiv 0; \tag{7}$$

(e) the pressure difference across the wing is*

$$\Delta p=p_- - p_+ = 2\rho\left(\frac{\partial\phi}{\partial t}+U\frac{\partial\phi}{\partial x}\right)_{z=0+}; \tag{8}$$

(f) the Kutta-Joukowsky condition of finite fluid velocity at the trailing-edge.

Here, S and W are the projections of the wing and wake onto the plane $z = o$, and R is the remaining part of this plane. It is assumed that vorticity is shed continually from the trailing edge with effect from $t = 0$ in such a way that the Kutta-Joukowsky condition is satisfied for $t \geqslant 0$.

The continuity of the downwash at the trailing edge has been considered by Leehey[4] for two-dimensional wings in arbitrary unsteady motion. He showed that continuity is a direct consequence of the Kutta-Joukowsky condition. R. T. Jones[6] applied this continuity property to determine, approximately, the initial forces on elliptic wings of high aspect ratio. In the present paper, we shall also make use of this property in order to analyse the initial forces and moments on wings of arbitrary planform and aspect ratio.

If the instantaneous downwash distribution over the wing and wake were known, the corresponding distribution of ϕ could be determined using Green's formula,

$$\phi(x,y,z,t)=\frac{1}{2\pi}\lim_{Z\to o}\iint_{S+W}\phi(X,Y,o,t)\frac{\partial}{\partial Z}\left(\frac{1}{r}\right)dX\,dY, \tag{9}$$

---

*The boundary value problem may be regarded as one for the half-space $z>o$ or $z<o$. From here onwards we consider the problem for $z>o$.

where $r^2 = (x-X)^2+(y-Y)^2+(z-Z)^2$, (X,Y,o) is any point inside $S+W$ and W is of length Ut. At each instant, the distribution of ϕ would be identical to that for steady flow without circulation over a wing of area $S+W$ and of given local incidence. Unfortunately, the downwash in the wake is not generally known in advance. An exception occurs just after the change of incidence when, by continuity, the downwash in the infinitesimal wake is $U\alpha$. Thus, at the initial instant, the distribution of ϕ over $S+W$ in the unsteady problem may be identified with that over a flat wing $S+W$ in a steady flow without circulation. This analogy with steady flow holds since the velocity potentials in both problems satisfy equations (3) and (6) together with the boundary condition

$$\frac{\partial \phi}{\partial z} = -U\alpha, \tag{10}$$

for points (x,y,o) inside $S+W$.

3. *Exact Applications of Analogy.*

On the basis of the previous section we now derive general formulae for the initial aerodynamic forces and moments on wings, following a sudden change of incidence. Some particular results are then obtained.

3.1. *Initial Forces and Moments.*

The total lift is given by

$$\left.\begin{aligned} L(t) &= 2\rho\iint_S \left(\frac{\partial \phi}{\partial t}+U\frac{\partial \phi}{\partial x}\right)dx\,dy = 2\rho\iint_{S+W}\left(\frac{\partial \phi}{\partial t}+U\frac{\partial \phi}{\partial x}\right)dx\,dy \\ &= 2\rho\frac{\partial}{\partial t}\iint_{S+W}\phi\,dx\,dy \end{aligned}\right\}, \tag{11}$$

since $\phi = 0$ at the edges of $S+W$. Similarly, the pitching moment about oy (Fig. 1a) is

$$M(t) = -2\rho\iint_S x\left(\frac{\partial \phi}{\partial t}+U\frac{\partial \phi}{\partial x}\right)dx\,dy = -2\rho\iint_{S+W} x\left(\frac{\partial \phi}{\partial t}+U\frac{\partial \phi}{\partial x}\right)dx\,dy$$

$$= -2\rho\frac{\partial}{\partial t}\iint_{S+W} x\phi\,dx\,dy + 2\rho U\iint_{S+W}\phi\,dx\,dy. \tag{12}$$

We now consider an instantaneous translation of the axes at time t to new origin o' where $oo' = \frac{1}{2}Ut$ and

$$x' = x-\tfrac{1}{2}Ut, \qquad y' = y, \qquad z' = z. \tag{13}$$

Thus, o' is the mid-root chord point of the wing $S+W$ (Fig. 1b). The initial values of $L(t)$ and $M(t)$ at $t = 0+$ can then be written

$$L_i = 2\rho\left[\frac{\Delta}{\Delta t}\iint_{S+W}\phi\,dx'dy'\right]_{t=0+}, \tag{14}$$

$$M_i = -2\rho\left[\frac{\Delta}{\Delta t}\iint\limits_{S+W} x'\phi dx'dy'\right]_{t=0+} + \rho U\left[\iint\limits_{S+W}\phi dx'dy'\right]_{t=0+}. \tag{15}$$

The integrals here are to be found from the solution for steady flow without circulation past the wing $S+W$. The operator $\Delta/\Delta t$ denotes that the derivatives are taken with origin of co-ordinates o' at the instantaneous mid-root chord position. Introduction of this form of differentiation is not strictly necessary in equation (14), but equation (15) is convenient for certain wings in Section 3.2 and for subsequent numerical applications.

There are corresponding formulae for the initial spanwise distribution of lift and pitching moment about oy;

$$l_i(y) = 2\rho\left[\frac{\Delta}{\Delta t}\int\limits_{x_0-\frac{1}{2}Ut}^{x_1+\frac{1}{2}Ut}\phi\, dx'\right]_{t=0+}, \tag{16}$$

$$m_i(y) = -2\rho\left[\frac{\Delta}{\Delta t}\int\limits_{x_0-\frac{1}{2}Ut}^{x_1+\frac{1}{2}Ut} x'\phi\, dx'\right]_{t=0+} + \rho U\left[\int\limits_{x_0-\frac{1}{2}Ut}^{x_1+\frac{1}{2}Ut}\phi\, dx'\right]_{t=0+}, \tag{17}$$

where $x = x_0(y)$, $x = x_1(y)$ are the equations of the leading and trailing edges. The initial chordwise distribution of lift is considered later in Section 8.

3.2. *Particular Results.*

We now give five simple results based on Section 3.1.

(i) In steady flow without circulation past a flat plate at small incidence α, we may replace the free stream U by a stream U parallel to the plate and a stream $U\alpha$ perpendicular to it. The quantity

$$N = 2\rho U\iint\phi\, dx\, dy = -2\rho U\iint x\frac{\partial\phi}{\partial x}dx\, dy \tag{18}$$

is the couple acting on the plate and tending to increase α. Clearly N is independent of the orientation of S with respect to the flow direction. Thus, for rectangular plates symmetrically placed with respect to the uniform flow and at incidence α,

$$\frac{C_N(A)}{A} = C_N(A') \qquad (AA' = 1), \tag{19}$$

where

$$C_N = \frac{N}{\frac{1}{2}\rho U^2 S c_r}.$$

Similarly, for elliptic plates,

$$\frac{C_N(A)}{A} = \frac{\pi}{4}C_N(A') \qquad \left[AA' = \left(\frac{\pi}{4}\right)^2\right]. \tag{20}$$

(ii) Consider the forces which act on a wing in forward and reverse flight after a sudden change of incidence from zero to α. According to Heaslet and Spreiter[13], the total lift forces at corresponding times are equal. That this is true for the initial lifts can be seen as follows. At corresponding times, the shapes and areas of $S+W$ are identical in forward and reverse flight. Just after the change of incidence the flow can be regarded as that past a flat plate $S+W$ and so the above invariant property of N can be used. It then follows immediately from equation (14) that the initial lift is the same in forward and reverse flight.

(iii) By combining the simple, basic ideas of (i) and (ii) and applying them to equation (16) it is seen that the initial spanwise distributions of lift are identical in forward and reverse flight. In general, this property will not remain true in the subsequent motion.

(iv) The initial pitching moment and its spanwise distribution for wings symmetrical with respect to oy simplify to

$$M_i = \rho U\left[\iint_{S+W} \phi\, dx'dy'\right]_{t=0+} = \tfrac{1}{2}N \tag{21}$$

and

$$m_i(y) = \rho U\left[\int_{x_0-\frac{1}{2}Ut}^{x_1+\frac{1}{2}Ut} \phi\, dx'\right]_{t=0+} = \tfrac{1}{2}n(y), \text{ say,} \tag{22}$$

since $S+W$ is symmetrical with respect to $o'y'$ and so ϕ is an even function of x'. Thus, for elliptic wings on which

$$\phi(x,y,o) = \frac{U\alpha a}{E}\left(1-\frac{x^2}{a^2}-\frac{y^2}{s^2}\right)^{\frac{1}{2}},$$

we find

$$M_i = \pi\rho U^2\alpha a^2 s\left(\frac{2}{3E}\right),\ m_i(y) = \pi\rho U^2\alpha a^2\left(\frac{1-y^2/s^2}{2E}\right),$$

where E is the ratio of semi-perimeter to span.

(v) For two-dimensional wings, where the distribution of ϕ over the chord is $U\alpha(a^2-x^2)^{\frac{1}{2}}$,

$$n = \pi\rho U^2\alpha a^2.$$

Application of equations (16) and (22) now gives for the initial lift and pitching moment

$$l_i = \frac{1}{U}\left(\frac{\Delta n}{\Delta t}\right)_{t=0+} = \pi\rho U\alpha\frac{\Delta}{\Delta t}(a^2) = \pi\rho U^2\alpha a$$

$$m_i = \tfrac{1}{2}n \qquad = \tfrac{1}{2}\pi\rho U^2\alpha a^2,$$

whence the initial position of the centre of lift is at the quarter-chord point. These results are in agreement with those derived in Refs. 1, 2 and 5.

4. *Approximate Equations for Steady Flow without Circulation.*

In order to be able to apply the formulae of Section 3.1 to the initial forces and moments on wings of arbitrary planform and aspect ratio, it is necessary to derive the solution for steady flow without circulation. The exact integral equation for this latter problem is first considered.

The perturbation velocity potential $\phi(x,y,z)$ for steady flow without circulation past a flat wing S is given by Green's formula as

$$\phi(x,y,z) = \frac{1}{2\pi} \lim_{Z \to o} \iint_S \phi(X,Y,o) \frac{\partial}{\partial Z}\left(\frac{1}{r}\right) dX\, dY.$$

On differentiation with respect to z and letting $z \to o$, it can be shown that the following two equivalent forms of integral equation hold for (x,y,o) inside S;

$$U\alpha = \frac{1}{2\pi} \frac{\partial}{\partial x} \iint_S \frac{\partial \phi}{\partial Y} \frac{[(x-X)^2+(y-Y)^2]^{\frac{1}{2}}}{(x-X)(y-Y)} dX\, dY, \tag{23}$$

$$U\alpha = \frac{1}{2\pi} \frac{\partial}{\partial y} \iint_S \frac{\partial \phi}{\partial X} \frac{[(x-X)^2+(y-Y)^2]^{\frac{1}{2}}}{(x-X)(y-Y)} dX\, dY, \tag{24}$$

where the integrals are to be interpreted as Cauchy principal values.

Unfortunately, the inversion formulae for these equations are not known for general planforms. Approximate equations, suitable for wings of high and of low aspect ratio, will be derived in Sections 4.1 and 4.2. Although more elaborate approximate methods are available we follow the lines of Lawrence[14] and reduce the double integral equations (23) and (24) to two single ones. It will be seen that there is a precise duality between the high-aspect-ratio and low-aspect-ratio approximations. This duality is not so apparent in Ref. 14 where steady flow with circulation is considered.

4.1. *Wings of High Aspect Ratio.*

We first multiply equation (23) by $2[x_1(y)-x]^{\frac{1}{2}}[x-x_0(y)]^{\frac{1}{2}}$ and integrate over the local chord to obtain

$$\tfrac{1}{4}\pi U\alpha c^2(y) = -\frac{1}{\pi} \int_{-s.}^{s.} dY \int_{x_0(Y)}^{x_1(Y)} \frac{\partial \phi}{\partial Y} dX \int_{x_0(y)}^{x_1(y)} \frac{[(x-X)^2+(y-Y)^2]^{\frac{1}{2}}}{(x-X)(y-Y)} \frac{\frac{1}{2}(x_0+x_1)-x}{[(x_1-x)(x-x_0)]^{\frac{1}{2}}} dx, \tag{25}$$

where $c(y) = x_1(y)-x_0(y)$. For wings of high aspect ratio $[(x-X)^2+(y-Y)^2]^{\frac{1}{2}}$ is approximately $|y-Y|$ over most of the platform. If this approximation is made, the integration with aspect to x gives $-\pi|y-Y|/(y-Y)$ and then equation (25) simplifies to

$$\tfrac{1}{4}\pi\rho U^2\alpha c^2(y) = 2\rho U \int_{x_0}^{x_1} \phi dX = n(y). \tag{26}$$

This is equivalent to the assumption that two-dimensional theory holds at each section y = constant [cf. Section 3.2, (v)]. We shall refer to this point in Section 10. If the approximation $[\frac{1}{4}c^2(y)+(y-Y)^2]^{\frac{1}{2}}$ is made for $[(x-X)^2+(y-Y)^2]^{\frac{1}{2}}$, equation (25) can be written in the form

$$\tfrac{1}{4}\pi\rho U^2\alpha c^2(y) = \tfrac{1}{2}n(y)+\tfrac{1}{4}\int_{-s}^{s}\frac{[\frac{1}{4}c^2(y)+(y-Y)^2]^{\frac{1}{2}}}{y-Y}\frac{dn}{dY}dY. \tag{27}$$

The analysis involved is too lengthy to be given here but the derivation is similar to Lawrence's derivation of equation (39) in Ref. 14. For rectangular wings, it can be shown that equation (27) holds exactly as aspect ratio tends to zero.

4.2. *Wings of Low Aspect Ratio.*

This time we start from equation (24) which we multiply by $2[\frac{1}{4}b^2(x)-y^2]^{\frac{1}{2}}$ and integrate over the local span. The procedure is then analogous to that of Section 4.1 and similar to that given by Lawrence[14] for the flow with circulation past wings of low aspect ratio. On using the approximation $|x-X|$ for $[(x-X)^2+(y-Y)^2]^{\frac{1}{2}}$, we obtain

$$\tfrac{1}{4}\pi\rho U^2\alpha b^2(x) = 2\rho U\int_{-\frac{1}{2}b}^{\frac{1}{2}b}\phi dY = h(x), \text{ say,}$$

analogous to equation (26). Similarly, on making the approximation $[(x-X)^2+\frac{1}{4}b^2(x)]^{\frac{1}{2}}$ for $[(x-X)^2+(y-Y)^2]^{\frac{1}{2}}$, we find that

$$\tfrac{1}{4}\pi\rho U^2\alpha b^2(x) = \tfrac{1}{2}h(x)+\tfrac{1}{4}\int_{-a}^{a}\frac{[(x-X)^2+\frac{1}{4}b^2(x)]^{\frac{1}{2}}}{x-X}\frac{dh}{dX}dX, \tag{28}$$

which is analogous to equation (27). For rectangular wings, it can be shown that equation (28) holds exactly as aspect ratio tends to infinity.

Equations (27) and (28) are identical in form. They are not, however, valid for every type of planform. For example, equation (28) cannot be used for swallow-tailed wings. On the other hand, use of this equation, unlike the corresponding equation in Lawrence's theory, is not restricted to wings with unswept trailing edges.

5. *Method of Solution for Wings of High Aspect Ratio.*

Equation (27) is an integro-differential equation for $n(y)$ which must satisfy

$$n(y) = n(-y) \quad \text{and} \quad n(\pm s) = 0.$$

Let $n(y) = n^*(\theta)$ and $c(y) = c^*(\theta)$, where $y = s\cos\theta$, and write

$$n^*(\theta) = \pi\rho U^2\alpha a^2\sum_{r=1}^{j}B_{2r-1}\frac{\sin(2r-1)\theta}{2r-1}, \tag{29}$$

where the coefficients B_{2r-1} are non-dimensional. It follows that

$$N = \int_{-s}^{s}n(y)dy = \tfrac{1}{2}\pi^2\rho U^2\alpha a^2 sB_1.$$

On substituting the series (29) into equation (27) we obtain

$$\left[\frac{c^*(\theta)}{a}\right]^2 = \sum_{r=1}^{j} B_{2r-1}\left\{\frac{2\sin(2r-1)\theta}{2r-1} - I_{2r-1}\right\}, \tag{30}$$

where

$$I_{2r-1} = \int_0^{\pi} \frac{[(c^*(\theta)/2s)^2 + (\cos\theta - \cos\bar{\theta})^2]^{\frac{1}{2}}}{\cos\theta - \cos\bar{\theta}} \cos(2r-1)\bar{\theta}.d\bar{\theta}.$$

This integral is written as

$$I_{2r-1} = \frac{c^*(\theta)}{2s}\int_0^{\pi} \frac{\cos(2r-1)\bar{\theta}}{\cos\theta - \cos\bar{\theta}}\, d\bar{\theta} + \int_0^{\pi} \frac{[(c^*(\theta)/2s)^2 + (\cos\theta - \cos\bar{\theta})^2]^{\frac{1}{2}} - c^*(\theta)/2s}{\cos\theta - \cos\bar{\theta}} \cos(2r-1)\bar{\theta}.d\bar{\theta}$$

The first integral can be integrated as a Cauchy principal value and the second can be written as a regular integral. Hence,

$$I_{2r-1} = \frac{-\pi c^*(\theta)}{2s}\,\frac{\sin(2r-1)\theta}{\sin\theta} + \int_0^{\pi} \frac{(\cos\theta - \cos\bar{\theta})\cos(2r-1)\bar{\theta}.d\bar{\theta}}{[(c^*(\theta)/2s)^2 + (\cos\theta - \cos\bar{\theta})^2]^{\frac{1}{2}} + c^*(\theta)/2s}.$$

The integral here can be evaluated numerically to any desired degree of accuracy. In the computations for equation (30), j was taken as 4 and the equation was satisfied at the 7 spanwise control points $\theta = \pi/8, 2\pi/8, \ldots 7\pi/8$. Before solving the matrix equation for B_{2r-1}, the accuracy is refined by introducing correction factors

$$\zeta_r = \frac{\sin\theta_r}{\theta_r}, \text{ where } \theta_r = \frac{(2r—1)\pi}{2j} (r = 1,2, \ldots j),$$

into those terms arising from $dn^*/d\theta$. This procedure is in accordance with Chapter 4 of Ref. 15. Values of the coefficients B_{2r-1} are given in Table 1 for rectangular and cropped delta wings.

6. *Method of Solution for Wings of Low Aspect Ratio.*
Equation (28) is an integro-differential equation for $h(x)$ which must satisfy

$$h(\pm a) = 0.$$

Let $h(x) = h^*(\psi)$ and $b(x) = b^*(\psi)$, where $x = a\cos\psi$, and write

$$h^*(\psi) = \pi\rho U^2 \alpha s^2 \sum_{r=1}^{k} D_r \frac{\sin r\psi}{r}, \tag{31}$$

where the coefficients D_r are non-dimensional. It follows that

$$N = \int_{-a}^{a} h(x)dx = \tfrac{1}{2}\pi^2 \rho U^2 \alpha a s^2 D_1.$$

On substituting the trigonometrical quantities into equation (28) we find

$$\left[\frac{b^*(\psi)}{s}\right]^2 = \sum_{r=1}^{k} D_r \left\{ \frac{2\sin r\psi}{r} + \frac{\pi b^*(\psi)\sin r\psi}{2a \quad \sin\psi} - \right.$$

$$\left. - \int_0^{\pi} \frac{(\cos\psi - \cos\bar{\psi})\cos r\bar{\psi} \,.\, d\bar{\psi}}{[(b^*(\psi)/2a)^2 + (\cos\psi - \cos\bar{\psi})^2]^{\frac{1}{2}} + b^*(\psi)/2a} \right\}. \tag{32}$$

For rectangular wings, $h(x)$ is an even function of x, so that $D_r = 0$ if r is even. Further, comparison of equation (30) with $c^*(\theta) \equiv 2a$ and of equation (32) with $b^*(\psi) \equiv 2s$ shows that they are equivalent if a and s are interchanged. Regarded as functions of aspect ratio,

$$B_{2r-1}(A) = D_{2r-1}(A') \quad (AA' = 1), \tag{33}$$

if the number and positions of the respective control points are the same. This simplification has been adopted and the results for $B_{2r-1}(A)$ used to give those for $D_{2r-1}(A')$. Thus, computations to find $h^*(\psi)$ for rectangular wings of low aspect ratio were effectively made with 7 chordwise control points, $\psi = \pi/8$, $2\pi/8$, ... $7\pi/8$.

Rather more care has been taken with the calculations for delta wings by the low-aspect-ratio method. For such wings, $h(x)$ is not an even function of x and equation (32) is satisfied at $(k-1)$ chordwise control points $\psi = \pi/k$, $2\pi/k$, ... $(k-1)\pi/k$, together with the apex condition

$$\sum_{r=1}^{k} (-1)^{r+1} D_r = 0.$$

Values of D_r are given in Tables 2 and 3 for delta wings of taper ratios $\lambda = 0$ and 1/7, with $k = 6$.

7. *Impulsive Load Distribution.*

The forces at $t = 0$ are of an impulsive nature due to the infinite acceleration of the wing and the assumed incompressibility of the fluid. The impulsive load distribution,

$$(\Delta p)_{t=0} = 2\rho \frac{\partial \phi}{\partial t} = 2\rho\phi(x,y,o)\frac{\partial}{\partial t}[1(t)],$$

is found from the velocity potential $\phi(x,y,o)$ for steady flow without circulation. For all wings symmetrical with respect to ox and oy the centre of lift is at the origin o for $t = 0$, whilst the impulsive loading vanishes at the edges of every wing.

The impulsive lift coefficient is

$$(C_L)_{t=0} = \frac{c_r C_N}{U}\delta(t), \tag{34}$$

where the coefficient C_N is defined in Section 3.2(i) and where $\delta(t)$ is the Dirac delta function

$$\left.\begin{aligned} \delta(t) &= 0 \quad (t \neq 0) \\ \delta(t) &= \infty \quad (t = 0) \\ \int_{-\infty}^{\infty} \delta(t)dt &= 1 \end{aligned}\right\}.$$

The spanwise distribution of impulsive loading is given by

$$\int_{x_0(y)}^{x_1(y)} (\Delta p)_{t=0}dx = \frac{n(y)}{U}\delta(t),$$

and the chordwise distribution by

$$\int_{-\frac{1}{2}b(x)}^{\frac{1}{2}b(x)} (\Delta p)_{t=0}dy = \frac{h(x)}{U}\delta(t).$$

Thus, for wings of high aspect ratio the spanwise distributions are obtainable from the results computed for equation (29); for wings of low aspect ratio the chordwise distributions are obtainable from the results computed for equation (31).

8. *Initial Load Distribution.*

In this section we give formulae for the initial forces and moments on delta wings of arbitrary taper ratio λ. These formulae may be applied immediately to rectangular wings with $\lambda = 1$. In Section 8.3 some special results are given for delta wings in reverse flight.

8.1. *Spanwise and Chordwise Loadings.*

In order to calculate the initial loading it is necessary to find solutions for steady flow without circulation past the planforms S and $S+W$. Since the semi-apex angle ε is the same for both, the chord of the wing S (Fig. 1) is expressed as

$$c^*(\theta) = 2a - (s\cot\varepsilon)|\cos\theta|, \tag{35}$$

so that the planform $S+W$ satisfies equation (35) if a is replaced by

$$a + \tfrac{1}{2}U\delta t = a + \delta a = a - \frac{a}{\sigma}\delta\sigma, \tag{36}$$

where $\sigma = s/a$. The coefficients B_{2r-1} and D_r may be regarded either as functions of A and λ or as functions of σ and ε.

On using equation (36) with formulae of Sections 3.1 and 5, we obtain results for delta wings of high aspect ratio. Thus, combined use of equations (16), (29) and (36) gives

$$C_{li}(y) = \frac{\pi a \alpha}{c(y)} \sum_{r=1}^{j} (2B_{2r-1} - \sigma B'_{2r-1}) \frac{\sin(2r-1)\theta}{2r-1}, \tag{37}$$

whence

$$C_{Li} = \frac{\pi^2 (2B_1 - \sigma B'_1)}{4(1+\lambda)} \alpha. \tag{38}$$

Dashes denote partial differentiation with respect to σ (ε constant). Equations (37) and (38) may be used to give the initial position of the spanwise centre of lift; thus,

$$\bar{\eta}_i = \frac{\sum_{r=1}^{j} J_{2r-1}(2B_{2r-1} - \sigma B'_{2r-1})}{2B_1 - \sigma B'_1},$$

where

$$(2r-1)J_{2r-1} = \frac{2}{\pi} \int_0^{\pi/2} \sin(2r-1)\theta \sin 2\theta . d\theta.$$

We note that the theoretical limit of B_1 as $A \to \infty$ is

$$\lim_{A \to \infty} B_1 = \frac{4(1+\lambda+\lambda^2)}{3\pi} = \frac{12 - 6\sigma \cot\varepsilon + \sigma^2 \cot^2 \varepsilon}{3\pi}, \tag{39}$$

and that use of this in equation (38) gives

$$\lim_{A \to \infty} C_{Li} = \pi\alpha,$$

in agreement with Wagner's result for two-dimensional wings.

Similarly, on using equation (36) with formulae of Sections 3.1 and 6, results are obtained for delta wings of low aspect ratio. The initial chordwise loading distribution is

$$g_i(x) = \int_{-\frac{1}{2}b(x)}^{\frac{1}{2}b(x)} \Delta p_i \, dy.$$

It is shown in the Appendix that the coefficient

$$C_{gi}(x) = \frac{g_i(x)}{\frac{1}{2}\rho U^2 b(x)} = \frac{-\pi\sigma s\alpha}{b(x)} \left[\tan\tfrac{1}{2}\psi \sum_{r=1}^{k} D_r \cos r\psi + \sigma \sum_{r=1}^{k} D'_r \frac{\sin r\psi}{r} \right], \tag{40}$$

where $D'_r = \partial D_r/\partial\sigma$. The total lift coefficient is then given by

$$C_{Li} = \frac{\pi^2\sigma(D_1 - \sigma D'_1)}{4(1+\lambda)}\alpha, \tag{41}$$

whilst the distance of the centre of lift from the apex is given as a fraction of root chord by

$$\overline{X}_i = \tfrac{1}{2} - \frac{C_{Mi}}{C_{Li}} = \frac{2D_2 - \sigma(4D'_1 + D'_2)}{8(D_1 - \sigma D'_1)}. \tag{42}$$

Use of the theoretical limits

$$\lim_{A\to 0} D_1 = \frac{4}{3\pi}(1+2\lambda) = \frac{4(3-\sigma\cot\varepsilon)}{3\pi} \tag{43}$$

and

$$\lim_{A\to 0} D_2 = \frac{8}{3\pi}(1-\lambda)(1+3\lambda) = \frac{2\sigma\cot\varepsilon(8-3\sigma\cot\varepsilon)}{3\pi} \tag{44}$$

in equations (41) and (42) gives

$$\lim_{A\to 0} C_{Li} = \tfrac{1}{2}\pi A\alpha$$

$$\lim_{A\to 0} \overline{X}_i = \tfrac{2}{3}(1-\lambda)$$

in agreement with Garrick's[16] slender-wing theory for unsteady motion.

8.2. *Special Results for Rectangular Wings.*

Formulae (37) to (44) apply also to rectangular wings for which $\lambda = 1$, $\sigma = A$, $\varepsilon = \frac{1}{2}\pi$ and $D_r = 0$ if r is even. The coefficients B_{2r-1} and D_{2r-1} are then functions of A only. For rectangular wings of high aspect ratio we have the additional formulae from use of equations (21) and (22),

$$C_{mi}(y) = \frac{\pi\alpha}{4}\sum_{r=1}^{j} B_{2r-1}\frac{\sin(2r-1)\theta}{2r-1}, \tag{45}$$

$$C_{Mi} = \frac{\pi^2 B_1}{16}\alpha, \tag{46}$$

so that

$$\overline{X}_i = \frac{B_1 - AB'_1}{2(2B_1 - AB'_1)}, \tag{47}$$

on using equation (38). The initial position of the local chordwise centre of pressure X_{cp} can be calculated from equations (37) and (45).

There is an exact solution for the initial position of the centre of lift for the square wing. Equation (47) becomes

$$\bar{X}_i(A) = \frac{B_1 - AB_1}{2(2B_1 - AB_1')} = \frac{C_N - AC_N'}{2(2C_N - AC_N')}$$

since $C_N = \frac{\pi^2}{8} B_1$ from Section 5. But, also,

$$C_N(A) = AC_N(1/A)$$

by equation (19). Hence,

$$2C_N'(1) = C_N(1), \tag{48}$$

and therefore

$$\bar{X}_i(1) = \frac{1}{6}. \tag{49}$$

8.3. *Special Results for Delta Wings.*

In Part II of this report we need to consider the flow past delta wings of low aspect ratio in reverse flight. Since the form of the function $h(x)$ is independent of flow direction, the chordwise loading distribution for a delta wing in reverse flight is

$$\left[c_{gi}(x)\right]_R = \frac{-\pi\sigma s\alpha}{b(x)} \left[\tan\tfrac{1}{2}\psi \sum_{r=1}^{k} D_r(-1)^{r+1} \cos r\psi + \sigma \sum_{r=1}^{k} D_r'(-1)^{r+1} \frac{\sin r\psi}{r}\right]; \tag{50}$$

the lift coefficient is still given by equation (41) whilst the position of the centre of lift is

$$\left[\bar{X}_i\right]_R = \frac{-2D_2 - \sigma(4D_1' - D_2')}{8(D_1 - \sigma D_1')}. \tag{51}$$

An important simplification can be introduced for complete delta wings ($\lambda = 0$) of low aspect ratio. We substitute $b^*(\psi) = 2a(1+\cos\psi)\tan\varepsilon$ in equation (32) and differentiate the resulting equation partially with respect to σ to give the analytical result

$$\sigma D_r' = -2D_r, \tag{52}$$

in place of simultaneous equations. We then find from equations (31), (40) and (52) that

$$2ag_i(x) = (a-x)h'(x) + 2h(x), \tag{53}$$

thus expressing the unsteady chordwise loading directly in terms of the solution for steady flow without circulation. The additional simple relationship for complete delta wings,

$$\bar{X}_i + \left[\bar{X}_i\right]_R = \frac{2}{3}, \tag{54}$$

is derived from equations (42), (51) and (52). This result, together with those of equations (52) and (53), is subject to the approximation of the low-aspect-ratio method, but can be shown to be exact when $A = 0$ and $A = \infty$.

9. *Numerical Results.*

For the high-aspect-ratio method the coefficients B_{2r-1} were computed at each value σ and also at $\sigma \pm 0{\cdot}01\sigma$, so that the derivatives B'_{2r-1} could be evaluated numerically. In the case of a delta wing, ε was kept constant for the three computations. Numerical results have been obtained for rectangular wings and for delta wings of taper ratio 1/7. Table 1 gives values of B_{2r-1} and $\sigma B'_{2r-1}$ as found by the high-aspect-ratio method of Section 5 with $j = 4$.

Calculations by the low-aspect-ratio method of Section 6 were made for complete and cropped delta wings ($\lambda = 0$ and 1/7). For $\lambda = 0$ the derivatives D'_r were found directly from the computed values of D_r by equation (52). For $\lambda = 1/7$ D'_r were obtained by differentiating equation (32) partially with respect to σ. Tables 2 and 3 give values of D_r and $\sigma D'_r$ for delta wings as found by the low-aspect-ratio method of Section 6 with $k = 6$. Values of D_{2r-1} and $\sigma D'_{2r-1}$ for rectangular wings ($\sigma = A$) can be found from equation (33) and Table 1. Numerical results for initial lift coefficients and the chordwise and spanwise centres of lift are given in Table 4.

9.1. *Accuracy of Results.*

As implied in Section 1, supreme accuracy has not been the objective of this paper. However, certain checks on the accuracy of the respective numerical methods have been made.

Two different checks were carried out on the high-aspect-ratio method. Firstly, the number of control points across the semi-span was increased from $j = 4$ to $j = 8$ for rectangular wings of aspect ratio 6 and 1. The differences in the leading coefficient B_1 were about 1 per cent at $A = 6$ and 0·1 per cent at $A = 1$, and similar differences were found in the initial lift coefficient. A similar check for the delta wing of aspect ratio 3 produced a difference of about 3 per cent in B_1, but the difference in the initial lift coefficient was only 1 per cent. The second check was performed by increasing the number of computations for a given wing to five in some cases (at σ ,$\sigma \pm 0{\cdot}01\sigma$, $\sigma \pm 0{\cdot}02\sigma$). However, use of the extra two computations showed insignificant changes in the derivatives B'_{2r-1}.

The effect of varying k in the low-aspect-ratio method is illustrated for delta wings in Table 5. It is seen that the values of initial lift and centre of lift are monotonic for the complete delta of aspect ratio $A = 1$ with a difference of about $2\frac{1}{2}$ per cent between the $k = 6$ and $k = 20$ solutions. These features hold, in fact, for all the complete deltas for which values have been computed. For $\lambda = 1/7$, the values fluctuate for $k \leqslant 20$, but are possibly monotonic for $k \geqslant 20$. This behaviour reflects that of the derivatives D'_1 and D'_2, since D_1 and D_2 remain monotonic in k for the cropped delta wings. The initial chordwise distributions of loading for the cropped delta wing $A = 0{\cdot}7$ with $k = 10$ are compared in Table 6 with corresponding quantities for $k = 20$, 40 and 60. In this respect the fluctuating behaviour of the solution shows no diminution with increasing k. For general planforms the differentiation of D_r must be carried out numerically. Therefore, some calculations were made in this way for cropped delta wings, but the results for both lift and chordwise loading distribution differed only very slightly from those found by differentiating equation (32) with respect to σ.

For rectangular wings of high aspect ratio the impulsive lift coefficient is

$$(C_L)_{t=0} = \tfrac{1}{4}\pi B_1(A)\left\{\frac{\pi c_r \alpha}{2U}\delta(t)\right\},$$

where the quantity in curly brackets is the two-dimensional result. Values of $\frac{1}{4}\pi B_1(A)$ as calculated by the present method for $A = 4$ and 6 agree to three decimal places with some results of W. P. Jones[17].

The coefficients B_1 and D_1 are both related to N (Sections 5 and 6) and should satisfy

$$B_1 = \sigma D_1. \tag{55}$$

For rectangular wings it follows from equation (33) that

$$B_1(A) = AB_1(1/A). \tag{56}$$

The results in Table 1 give a good approximation to equation (56) when $A = 2$ and 4. For cropped delta wings, Tables 1 and 3 show that equation (55) is well approximated when $A = 3$ but not when $A = 2$. This discrepancy can probably be attributed to the fact that, for non-rectangular wings, equations (27) and (28) remain approximate when $A \to 0$ and when $A \to \infty$ respectively.

9.2. *Initial Forces and Moments.*

Values of the initial lift coefficient C_{Li} for rectangular and delta wings from Table 4 are plotted against aspect ratio in Fig. 2. It is seen that all the values are less than $\frac{1}{2}\pi A$, the value given by Garrick's slender-wing theory; this is inconsistent with Lehrian's[11] result for the delta wing of taper ratio $\lambda = 1/7$ with $A = 1{\cdot}2$. For higher aspect ratios, the calculated initial lift coefficients of delta wings appear to be unreliable (*see* end of last section).

Fig. 3 shows curves of initial chordwise load distributions for rectangular wings, plotted against $\xi = \frac{1}{2} + x/c_r$. It is seen that the loading is slightly negative on a small strip near the trailing edge for $A = 0{\cdot}5$[†]. Initial chordwise load distributions for complete delta wings are shown in Fig. 4. The curves necessarily pass through the origin because the apex condition of Section 6 has been satisfied. In Fig. 5 the convergence of the initial chordwise loading on the complete delta $A = 1$ is shown and can be regarded as quite satisfactory.

It is of interest to compare the values of C_{Li}, as calculated for a given wing by the methods for high and low aspect ratios. For rectangular wings it is clear from the approximations in equations (27) and (28) that the dividing line should be $A = 1$; this is illustrated in the remarks preceding equation (33). It can be seen from Table 4 that the results from both methods agree well between $A = 0{\cdot}5$ and $A = 4$. The results predicted by both methods for the initial chordwise centre of lift $\bar{X}_i$ for the square wing are in excellent agreement with equation (49), but such agreement is perhaps a little fortuitous. For delta wings, the low-aspect-ratio method is thought to be satisfactory for $A \leqslant 2$.

10. *Comparisons between Initial and Final Values.*

We now compare the calculated initial values with the final, steady-state values attained at time $t = \infty$. Of course, several methods exist for steady flow but we have chosen the lifting-surface theory of Multhopp[18], since it is known to be reasonably accurate and is valid for a wide range of planform. It might be argued that, for high aspect ratios, we should compare with Weissinger's[19] theory since the method of Section 5 and Ref. 19 both use the approximation of equation (27). There is, however, the vital difference that, unlike that of Weissinger, the present method does not fix the local centre of pressure along the quarter-chord line. Again, it might be argued that, for low aspect ratios we should compare with Lawrence's[14] theory, since the method of Section 6 and Ref. 14 both use the approximation of equation (28). However, comparison of Goodman's[20] calculations by Lawrence's method ($k = 6$) and those in Table 7 by Multhopp's theory show satisfactory agreement.

Values of the final lift coefficient C_{Lf} from Table 7 are used to plot the ratio of initial lift to final lift against aspect ratio in Fig. 6. Good agreement is reached with the results of W. P. Jones[8] for the rectangular wings $A = 4$ and $A = 6$, and with the analogue calculations of Duquenne[12] for the rectangular wings $A = 1$ and $A = 3$. There are, however, significant discrepancies with Duquenne's results for $A \leqslant 0{\cdot}5$ and with Lehrian's[11] results for $2 \leqslant A \leqslant 4$. For very low-aspect-ratios the sign of $C_{Lf} - C_{Li}$ depends critically on the particular value chosen for C_{Lf}. For moderate aspect ratios it seems likely that Lehrian's results are somewhat inaccurate. The present results show that the ratio C_{Li}/C_{Lf} is usually greater for delta than for rectangular wings, at a fixed aspect ratio. The values given by Lehrian are much higher than those given here, especially for the cropped delta of aspect ratio $A = 1{\cdot}2$. For complete delta wings, the present values of C_{Li} suggest that the ratio C_{Li}/C_{Lf} does not exceed unity as aspect ratio tends to zero.

Initial and final spanwise loadings for the rectangular wing $A = 4$ are shown in Fig. 7, and the limiting distributions from two-dimensional strip theory and slender-wing theory indicate the extremes of aspect

---

[†] The same is true in the case $A = 0{\cdot}25$.

ratio. Drischler[9] has already shown that the spanwise distribution is, for all practical purposes, independent of time for rectangular wings when $Ut/c_r > 1$. The present results extend this feature to very small time; furthermore, the small difference between initial and final loadings for $A = 4$ in Fig. 7 becomes insignificant at $A = 1$. For general aspect ratio there is a weak discontinuity at $t = 0$ from the impulsive to the initial load distribution; there is then a gradual movement from the initial to the final distribution. This type of behaviour has also been shown by Vogel[7], although his results appear to be somewhat inaccurate when Ut/c_r is small. The initial chordwise loading by the method of Section 6 and the final chordwise loading from Ref. 20 for the rectangular wing $A = 4$ are shown in Fig. 8. The differences are very small and become insignificant as A decreases to 1. However, for general aspect ratio there is a strong discontinuity from the impulsive to the initial load distribution. Although the chordwise centre of lift $\bar{X}$ changes rapidly as aspect ratio decreases, Fig. 9 shows that the difference between the initial and final values, $\bar{X}_i - \bar{X}_f$, remains small. In Fig. 10 the differences between the spanwise centres of lift, $\bar{\eta}_i$ and $\bar{\eta}_f$, are comparable with the variations due to change of aspect ratio, but they remain small. The initial and final distributions of local centre of pressure are shown in Fig. 11 for two rectangular wings; the differences are fairly small for $A = 4$ and negligibly so for $A = 1$.

Initial and final spanwise loadings for the cropped delta wing $A = 3$ are given in Fig. 12, together with the limiting loadings from two-dimensional strip theory and slender-wing theory. At $t = 0$, there is a strong discontinuity in the spanwise loading distribution. The author knows of no results for intermediate time but it seems likely that the same features will apply as for rectangular wings, namely that the distribution will change gradually from its initial position to its final position. The present results for the lower aspect ratio $A = 2$ confirm that the initial and final loadings converge as A decreases. Initial and final chordwise loading distributions for the cropped delta wing $A = 3$ are shown in Fig. 13, the latter being obtained from a special integration of the wing loading calculated by Multhopp's lifting-surface theory. The difference here is not insignificant, but whether or not this is due to the inaccuracies in the present method requires further investigation. There is again a strong discontinuity in chordwise loading at $t = 0$. The initial chordwise centres of lift $\bar{X}_i$ for complete and cropped delta wings and the spanwise centre of lift $\bar{\eta}_i$ for cropped delta wings are given in Table 4; $\bar{X}_i$ and $\bar{X}_f$ are compared against aspect ratio in Fig. 14.

One feature of the present results obtained by the high-aspect-ratio method is that the initial values of all aerodynamic quantities are closer to the values predicted by two-dimensional strip theory than are the final values. This may be seen from Tables 4 and 7 and from each of the Figs. 6 to 13. This conclusion might have been anticipated in Section 4.1, since the result of replacing $[(x-X)^2+(y-Y)^2]^{\frac{1}{2}}$ by $|y-Y|$ led to the strip-theory equation (26) and would have shown no effects of finite span on the initial forces and moments. However, the result of making the identical approximation in the corresponding theory for steady flow with circulation leads to Prandtl's lifting-line equation and consequent prediction of finite-span effects.

11. *Acknowledgements.*

The author is indebted to Mr. C. T. H. Baker for programming the matrix calculations for the Mercury computer at Oxford University Computing Laboratory and for suggesting the inclusion of the correction factors mentioned in Section 5. Mrs. S. Lucas of the Aerodynamics Division, N.P.L., carried out the remaining calculations and prepared the tables and figures.

LIST OF SYMBOLS

a	Half root chord
A	Aspect ratio ($= 4s^2/S$)
$\bar{b}$	Mean span ($= S/2a$)
$b(x)$	Local span
B_{2r-1}	Fourier coefficients in equation (29)
B'_{2r-1}	$\partial B_{2r-1}/\partial\sigma$ (ε constant)
$\bar{c}$	Mean chord ($= S/2s$)
c_r	Root chord
$c(y)$	Local chord
C_L	Lift coefficient ($= L/\frac{1}{2}\rho U^2 S$)
C_M	Pitching moment coefficient ($= M/\frac{1}{2}\rho U^2 S c_r$)
C_N	$N/\frac{1}{2}\rho U^2 S c_r$
C_g	$g(x)/\frac{1}{2}\rho U^2 b(x)$
C_l	$l(y)/\frac{1}{2}\rho U^2 c(y)$
C_m	$m(y)/\frac{1}{2}\rho U^2 c^2(y)$
D_r	Fourier coefficients in equation (31)
D'_r	$\partial D_r/\partial\sigma$ (ε constant)
$g(x)$	Lift per unit chord
$h(x)$	Defined in Section 4.2
$l(y)$	Lift per unit span
L	Lift force on wing
$m(y)$	Pitching moment per unit span (about $x = o$)
M	Pitching moment (about $x = o$)
$n(y)$	Pitching moment N per unit span
N	Pitching moment relating to flow without circulation
p	Pressure
s	Maximum semi-span of wing
S	Projection uf planform onto $z = o$
t	Time
U	Velocity of free stream
W	Projection of wake onto $z = o$
$x_0(y)$	Ordinate of leading edge
$x_1(y)$	Ordinate of trailing edge
x,y,z	Right-handed co-ordinate system fixed in wing (Fig. 1a)
X_{cp}	$\frac{1}{2} - C_m/C_l$
$\bar{X}$	Centre of lift in equation (42)
α	Incidence
$\delta(t)$	Dirac delta function
ε	Semi-apex angle of delta wing
η	Non-dimensional spanwise co-ordinate ($= y/s$)
$\bar{\eta}$	Spanwise centre of lift for a half-wing
λ	Taper ratio (Fig. 1a)
ξ	Non-dimensional chordwise co-ordinate ($\frac{1}{2} + x/c_r$)
ρ	Density
σ	s/a
ϕ	Perturbation velocity potential
f	Subscript denoting final value
i	Subscript denoting initial value
$1(t)$	Unit step-function in equation (2)

REFERENCES

No.	*Author(s)*	*Title, etc.*
1	Th. von Kármán and W. R. Sears	Airfoil theory for non-uniform motion. *J. Aero. Sci.*, Vol. 5. August, 1938.
2	H. Söhngen	Bestimmung der Auftriebsverteilung für beliebige instationäre Bewegungen (Ebenes Problem). Luftfahrtforschung, Vol. 17, 1940.
3	W. R. Sears	Operational methods in the theory of airfoils in non-uniform motion. *J. Franklin Inst.*, Vol. 230. July, 1940.
4	P. Leehey	The Hilbert problem for an airfoil in unsteady flow. Navy Dept., David W. Taylor Model Basin, Report 1077. January, 1957.
5	H. Wagner	Über die Entstehung des dynamischen Auftriebes von Tragflügeln. Z.A.M.M., Vol. 5, 1925.
6	R. T. Jones	The unsteady lift of a wing of finite aspect ratio. N.A.C.A. Report No. 681, 1940.
7	U. Vogel	Ein Traglinienverfahren zur Berechnung der Auftriebsverteilung von Tragflügeln bei zeitabhängiger Vertikalbewegung. Z. Flugwiss., Vol. 12. April, 1964.
8	W. P. Jones	Aerodynamic forces on wings in non-uniform motion. A.R.C. R. and M.2117. August, 1945.
9	J. A. Drischler	Approximate indicial lift functions for several wings of finite span in incompressible flow as obtained from oscillatory lift coefficients. N.A.C.A. Tech. Note 3639. May, 1956.
10	I. E. Garrick	On some reciprocal relations in the theory of non-stationary flows. N.A.C.A. Report No. 629. 1938.
11	D. E. Lehrian	Initial lift of finite aspect ratio-wings due to a sudden change of incidence. A.R.C. R. and M. 3023. May, 1955.
12	R. Duquenne	Étude par analogie électrique des surfaces portantes en régime instationnaire. O.N.E.R.A. Publication No. 98. 1960.
13	M. A. Heaslet and J. R. Spreiter	Reciprocity relations in aerodynamics. N.A.C.A. Report No. 1119. 1953.
14	H. R. Lawrence	The lift distribution of low-aspect-ratio wings at subsonic speeds. *J. Aero. Sci.*, Vol. 18. October, 1951.
15	C. Lanczos	*Applied Analysis* (Pitman).

16 I. E. Garrick .. .. .. *Some research on high speed flutter.* Anglo-American Aeronautical Conference. Brighton. 1951. Lewes Press (Wightman and Co. Ltd.)

17 W. P. Jones .. .. .. Calculation of additional mass and inertia coefficients for rectangular plates in still air. A.R.C. R. and M. 1947. November, 1941.

18 H. Multhopp .. .. .. Methods for calculating the lift distribution of wings (Subsonic lifting-surface theory). A.R.C. R. and M. 2884. January, 1950.

19 J. Weissinger .. .. .. Über die Auftriebsverteilung von Pfeilflügeln. Z.W.B. (Berlin), F.B.1553. 1942.

20 Th. R. Goodman .. .. Calculation of aerodynamic characteristics of low-aspect-ratio wings at subsonic speeds. Cornell Aero. Lab. Report. August, 1951.

APPENDIX

Calculation of the Initial Chordwise Loading

The spanwise integral of loading at a section x = constant is

$$g_i(x) = 2\rho \int_{-\frac{1}{2}b(x)}^{\frac{1}{2}b(x)} \left(\frac{\partial \phi}{\partial t} + U\frac{\partial \phi}{\partial x}\right)_{t=0+} dy.$$

The method for wings of low aspect ratio gives

$$g_i(x) = 2\rho \int_{-\frac{1}{2}b(x)}^{\frac{1}{2}b(x)} \left(\frac{\partial \phi}{\partial t}\right)_{t=0+} dy + h'(x), \tag{A1}$$

where, by equation (31),

$$h(x) = \pi\rho U^2 \alpha s^2 \sum_{r=1}^{k} D_r \frac{\sin r\psi}{r}, \tag{A2}$$

and

$$h'(x) = \frac{-1}{a\sin\psi}\frac{dh^*}{d\psi} = \frac{-\pi\rho U^2\alpha s^2}{a\sin\psi}\sum D_r \cos r\psi. \tag{A3}$$

There are two contributions to $g_i(x)$ from the integral in equation (A1). One is

$$\frac{-\pi\rho U^2\alpha s^2}{2a}\sum\sigma D_r'\frac{\sin r\psi}{r}. \tag{A4}$$

The other arises from the terms $\sin r\psi$ in equation (A2) and is found by using the operator $\Delta/\Delta t$ (Section 3), bearing in mind that the operation takes place at a fixed point x on the wing root chord. However, it is first convenient to write

$$\sum D_r\frac{\sin r\psi}{r} = \sum_{r\ \text{odd}}\overline{D}_r\sin^r\psi + \sum_{r\ \text{even}}\overline{D}_r\sin^{r-1}\psi\cos\psi$$

where the $\overline{D}_r$ are linear combinations of the D_r. Recalling that $x = a\cos\psi$ and applying the operator to $\sin^r\psi$ and $\sin^{r-1}\psi\cos\psi$, we obtain

$$\frac{\Delta}{\Delta t}(\sin^r\psi) = \frac{rU}{2a}\frac{\sin^r\psi\cos\psi}{1-\cos\psi},$$

$$\frac{\Delta}{\Delta t}(\sin^{r-1}\psi\cos\psi) = \frac{U}{2a}\frac{\sin^{r-1}\psi(r\cos^2\psi-1)}{1-\cos\psi}.$$

Thus, the total contribution from the terms $\sin r\psi$ in $\Sigma D_r\dfrac{\sin r\psi}{r}$ is

$$\frac{U}{2a}\frac{\sin\psi}{1-\cos\psi}\left\{\sum_{r\ \text{odd}}\overline{D}_r r\sin^{r-1}\psi\,.\cos\psi + \sum_{r\ \text{even}}\overline{D}_r\sin^{r-2}\psi([r-1]-r\sin^2\psi)\right\}$$

which equals

$$\frac{U}{2a}\frac{\sin\psi}{1-\cos\psi}\Sigma D_r\cos r\psi. \tag{A5}$$

Hence, from (A3), (A4) and (A5),

$$C_{gi}(x) = \frac{g_i(x)}{\frac{1}{2}\rho U^2 b(x)}$$

$$= \frac{-\pi\sigma s\alpha}{b(x)}\left[\tan\tfrac{1}{2}\psi\Sigma D_r\cos r\psi + \sigma\Sigma D_r'\frac{\sin r\psi}{r}\right],$$

on combining (A3) and (A5).

In the case of two-dimensional wings, the distribution of ϕ over the chord for flow without circulation is $U\alpha[a^2-x^2]^{\frac{1}{2}}$, so that

$$\Delta p_i = 2\rho\left(\frac{\partial\phi}{\partial t}+U\frac{\partial\phi}{\partial x}\right)_{t=0+}$$

$$= 2\rho U^2\alpha\left(\tfrac{1}{2}\left[\frac{a+x}{a-x}\right]^{\frac{1}{2}}-\frac{x}{[a^2-x^2]^{\frac{1}{2}}}\right)$$

$$= \rho U^2\alpha\left[\frac{a-x}{a+x}\right]^{\frac{1}{2}},$$

which is one-half of the steady-state value. This is in agreement with Söhngen's[2] result.

TABLE 1

B_{2r-1} and $\sigma B'_{2r-1}$ for Rectangular and Delta Wings

(a) Values of B_{2r-1}

Planform	A	B_1	B_3	B_5	B_7
Rectangle ($\lambda = 1$)	6	1·140	0·495	0·050	−0·033
	4	1·095	0·391	0·034	−0·017
	3	1·049	0·310	0·026	−0·008
	2	0·957	0·203	0·019	−0·001
	1	0·733	0·078	0·010	0·002
	0·5	0·480	0·025	0·004	0·001
	0·25	0·277	0·007	0·001	0·000
Delta ($\lambda = 1/7$)	3	0·428	−0·433	0·253	−0·118
	2	0·382	−0·336	0·165	−0·073

(b) Values of $\sigma B'_{2r-1}$

Planform	A	$\sigma B'_1$	$\sigma B'_3$	$\sigma B'_5$	$\sigma B'_7$
Rectangle ($\lambda = 1$)	6	0·085	0·076	0·009	−0·006
	4	0·139	0·092	0·006	−0·005
	3	0·187	0·094	0·004	−0·004
	2	0·265	0·080	0·003	−0·002
	1	0·366	0·040	0·002	0·000
	0·5	0·344	0·044	0·007	0·001
	0·25	0·237	0·013	0·002	0·000
Delta ($\lambda = 1/7$)	3	−0·313	−0·237	0·099	−0·033
	2	−0·243	−0·215	0·069	−0·019

TABLE 2

D_r and $\sigma D'_r$ for Complete Delta Wings ($\lambda = 0$)

(a) Values of D_r

A	D_1	D_2	D_3	D_4	D_5	D_6
0·5	0·366	0·663	0·424	0·204	0·110	0·033
1	0·318	0·520	0·236	0·062	0·030	0·001
2	0·254	0·356	0·089	0·005	0·013	—0·005
4	0·182	0·209	0·015	0·003	0·005	—0·010

(b) Values of $\sigma D'_r$

A	$\sigma D'_1$	$\sigma D'_2$	$\sigma D'_3$	$\sigma D'_4$	$\sigma D'_5$	$\sigma D'_6$
0·5	−2·924	−5·302	−3·392	−1·634	−0·881	−0·262
1	−1·272	−2·081	−0·945	−0·249	−0·119	−0·005
2	−0·508	−0·711	−0·177	−0·009	−0·026	0·010
4	−0·182	−0·209	−0·015	−0·003	−0·005	0·010

TABLE 3

D_r and $\sigma D'_r$ for Cropped Delta Wings ($\lambda = 1/7$)

(a) Values of D_r

A	D_1	D_2	D_3	D_4	D_5	D_6
0·5	0·458	0·774	0·377	0·075	0·004	−0·010
0·7	0·427	0·687	0·275	0·016	−0·019	−0·021
1·2	0·367	0·529	0·132	−0·030	−0·019	−0·019
2	0·299	0·378	0·042	−0·028	−0·009	−0·019
3	0·243	0·273	0·004	−0·014	−0·009	−0·020

(b) Values of $\sigma D'_r$

A	$\sigma D'_1$	$\sigma D'_2$	$\sigma D'_3$	$\sigma D'_4$	$\sigma D'_5$	$\sigma D'_6$
0·5	−0·736	−0·941	0·291	1·101	0·990	0·385
0·7	−0·708	−0·892	0·252	0·907	0·782	0·310
1·2	−0·632	−0·744	0·224	0·617	0·483	0·203
2	−0·529	−0·559	0·205	0·382	0·288	0·141
3	−0·437	−0·413	0·178	0·242	0·197	0·109

TABLE 4

Initial Values of Lift and Centres of Lift*

Planform	A	$\frac{1}{\alpha}C_{Li}$		$\bar{X}_i$		$\bar{\eta}_i$
		High A	Low A	High A	Low A	High A
Rectangle ($\lambda = 1$)	6	2·708		0·240	—	0·453
	4	2·532	(2·536)	0·233	(0·231)	0·445
	3	2·357	—	0·226	—	0·439
	2	2·035	(2·032)	0·210	(0·209)	0·433
	1	1·358	1·357	0·167	0·167	0·427
	0·5	(0·759)	0·754	(0·110)	0·108	0·425
	0·25	(0·390)	0·381	(0·063)	0·056	0·425
Delta ($\lambda = 0$)	4	—	(2·696)	—	0·525	—
	2	—	1·880	—	0·567	—
	1	—	1·177	—	0·606	—
	0·5	—	0·676	—	0·636	—
Delta ($\lambda = 1/7$)	3	2·525	2·496	—	0·492	0·413
	2	(2·174)	2·034	—	0·513	0·422
	1·2	—	1·481	—	0·539	—
	0·7	—	0·992	—	0·561	—
	0·5	—	0·751	—	0·571	—

*Calculated values from the methods of Sections 5 and 6 are denoted by 'High A' and 'Low A' respectively. In plotting the results, those in brackets have been discarded as being the less accurate.

TABLE 5

Convergence of the Low-Aspect-Ratio Method for Delta Wings

k	$A = 1, \lambda = 0$		$A = 0{\cdot}7, \lambda = 1/7$		$A = 3, \lambda = 1/7$	
	$\frac{1}{\alpha}C_{Li}$	$\bar{X}_i$	$\frac{1}{\alpha}C_{Li}$	$\bar{X}_i$	$\frac{1}{\alpha}C_{Li}$	$\bar{X}_i$
6	1·177	0·606	0·981	0·561	2·519	0·497
7	1·170	0·602	1·026	0·573	2·576	0·503
10	1·159	0·596	0·968	0·554	2·471	0·490
20	1·150	0·591	0·992	0·561	2·496	0·492
40	—	—	0·975	0·554	—	—
60	—	—	0·969	0·552	—	—

TABLE 6

Initial Chordwise Loading on a Delta Wing ($A = 0{\cdot}7$, $\lambda = 1/7$) for Various Numbers of Control Points

ξ	Values of $\frac{bC_{gi}}{\overline{bC}_{Li}}$ for			
	$k = 10$	$k = 20$	$k = 40$	$k = 60$
0·024	0·055	0·072	−0·045	−0·070
0·095	0·292	0·341	0·217	0·379
0·206	0·659	0·688	0·615	0·708
0·345	1·080	1·082	1·040	1·102
0·500	1·476	1·443	1·423	1·467
0·655	1·653	1·631	1·617	1·640
0·794	1·613	1·465	1·468	1·435
0·905	0·326	0·450	0·579	0·484
0·976	0·236	0·180	0·213	0·185

TABLE 7

Final Values by Lifting Surface Theory (Ref. 18)

Planform	A	$\frac{1}{\alpha}C_{Lf}$	$\overline{X}_f$	$\bar{\eta}_f$
Rectangle ($\lambda = 1$)	6*	4·21	0·236	0·444
	4	3·601	0·228	0·436
	3*	3·16	0·221	0·432
	2	2·478	0·208	0·428
	1	1·461	0·167	0·426
	0·5	0·774	0·112	0·425
	0·25	0·392	0·069	0·424
Delta ($\lambda = 1/7$)	3	3·099	0·527	0·422
	2	2·394	0·539	0·424
	1·2	1·626	0·555	0·425
	0·7	1·024	0·569	0·425
	0·5	0·754	0·574	0·424

*Results for these wings have been estimated.

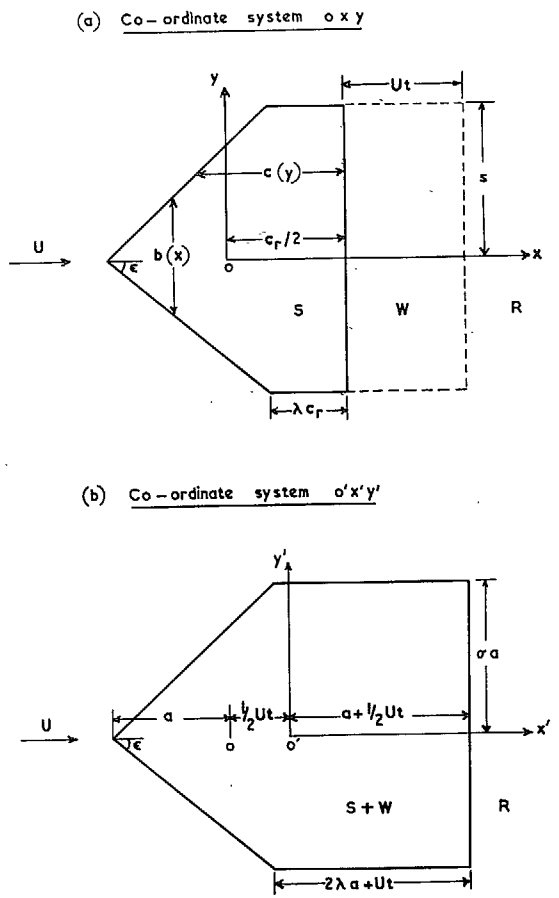

FIG. 1. Co-ordinate systems and definitions

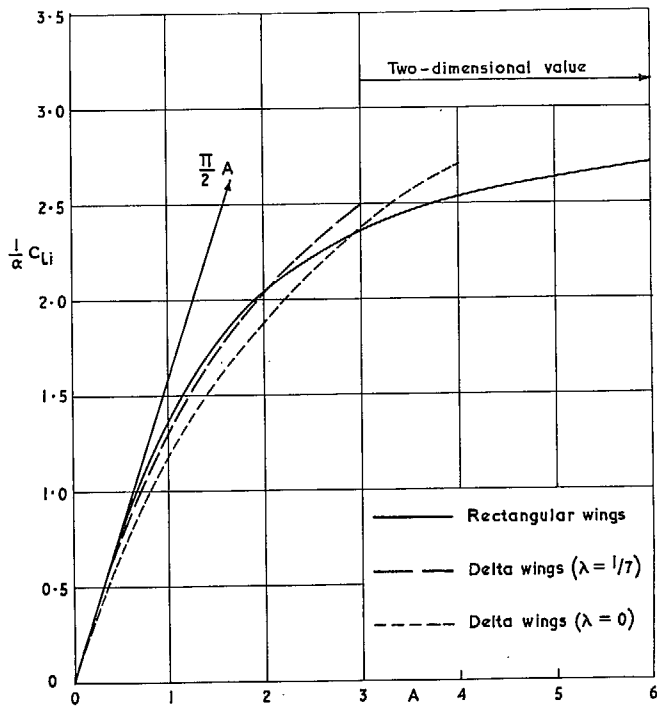

FIG. 2. Initial lift coefficient for rectangular and delta wings

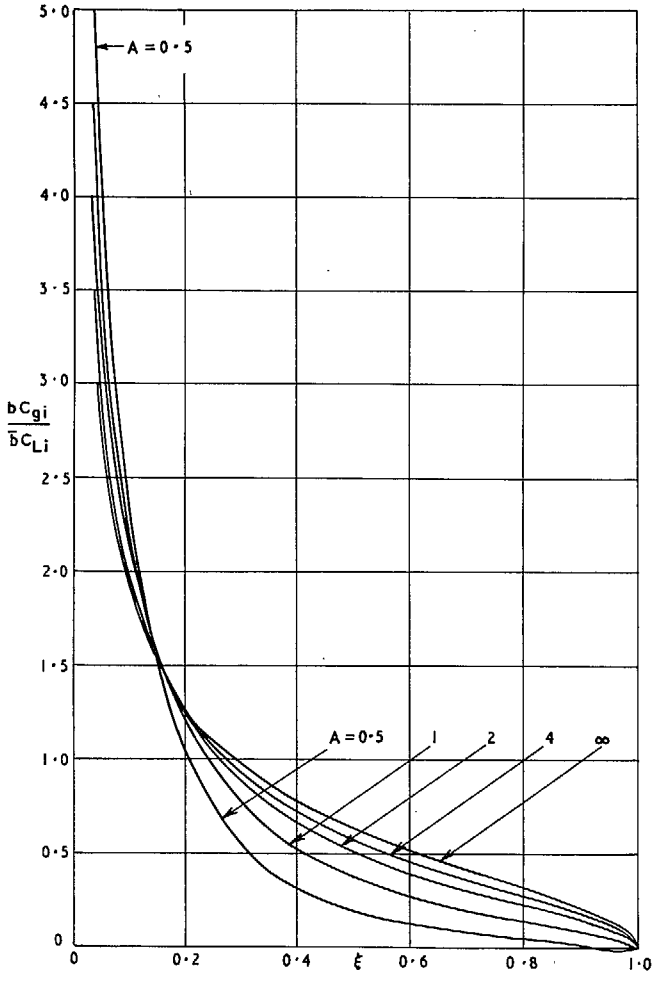

FIG. 3. Initial chordwise loading on rectangular wings.

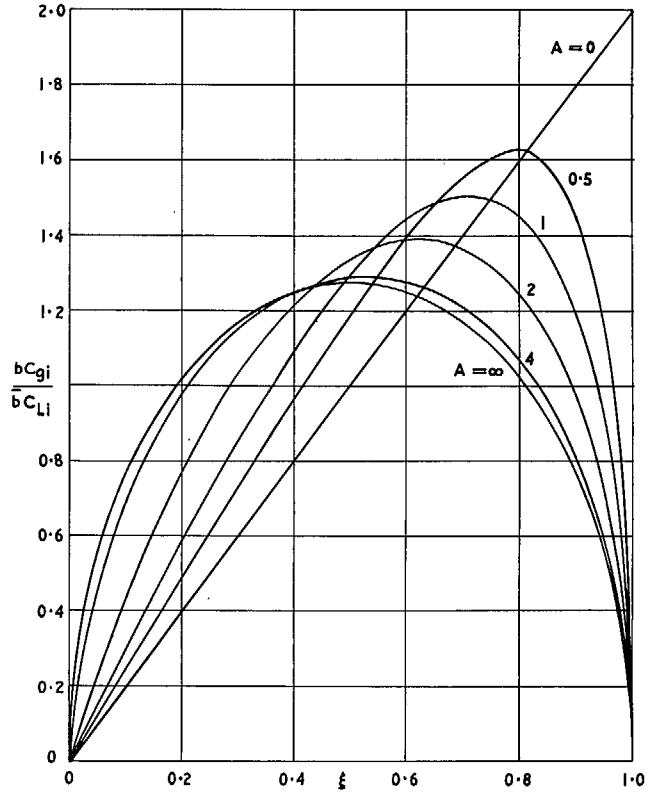

FIG. 4. Initial chordwise loading on delta wings ($\lambda = 0$)

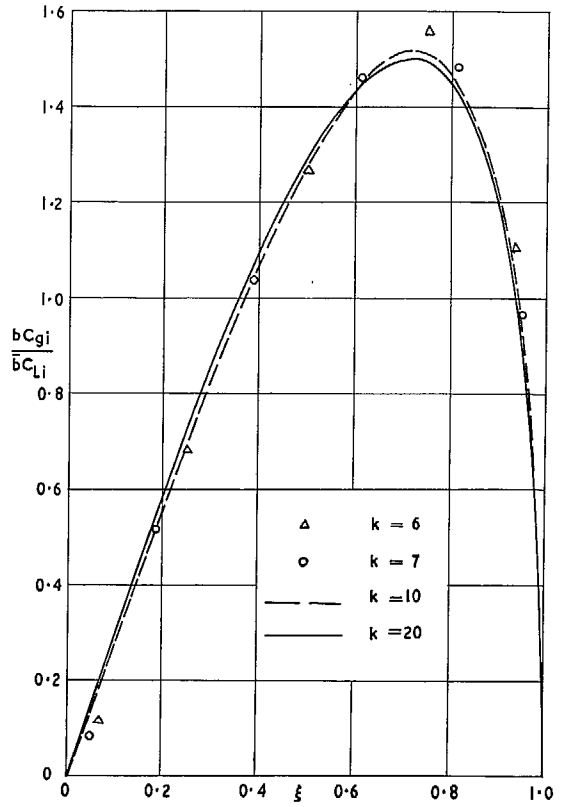

FIG. 5. Initial chordwise loading on a delta wing ($A = 1, \lambda = 0$) for various numbers of control points

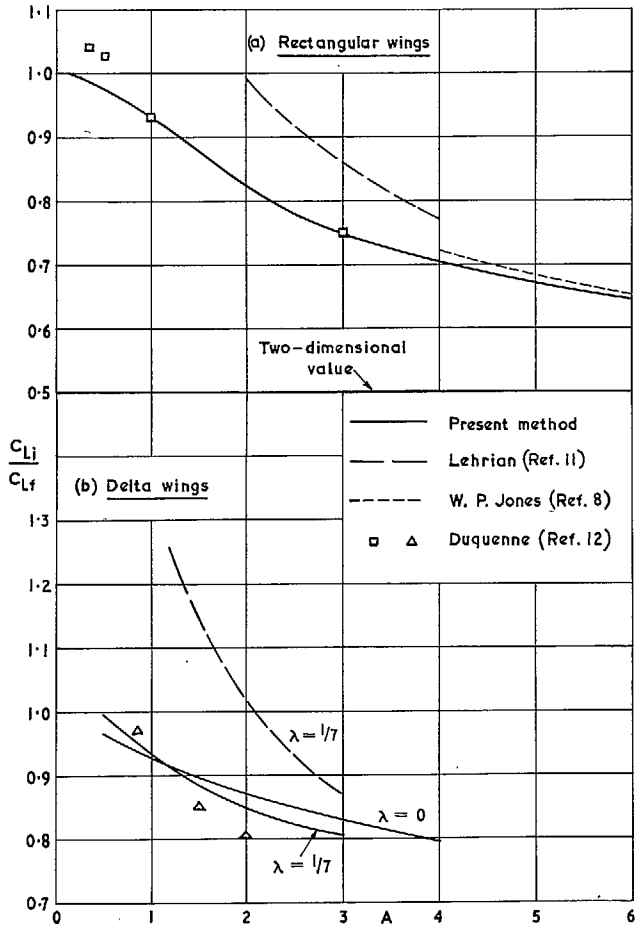

FIG. 6. Ratio of initial lift to final lift against aspect ratio.

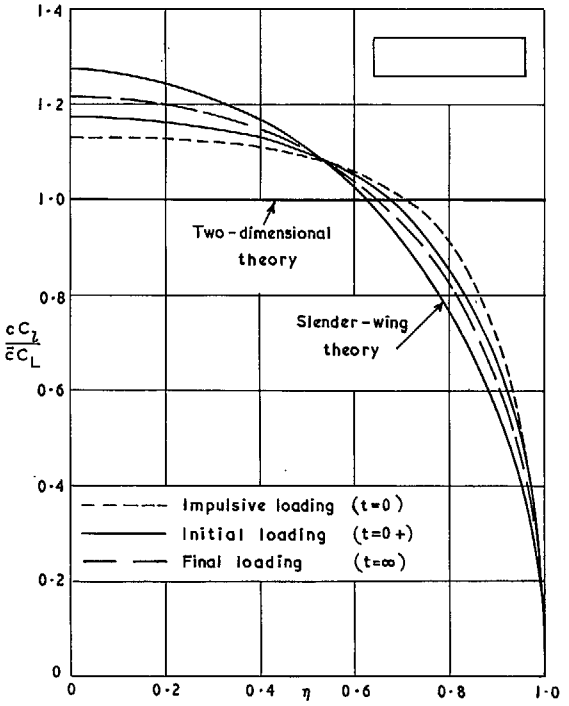

FIG. 7. Initial and final spanwise loading on a rectangular wing ($A = 4$)

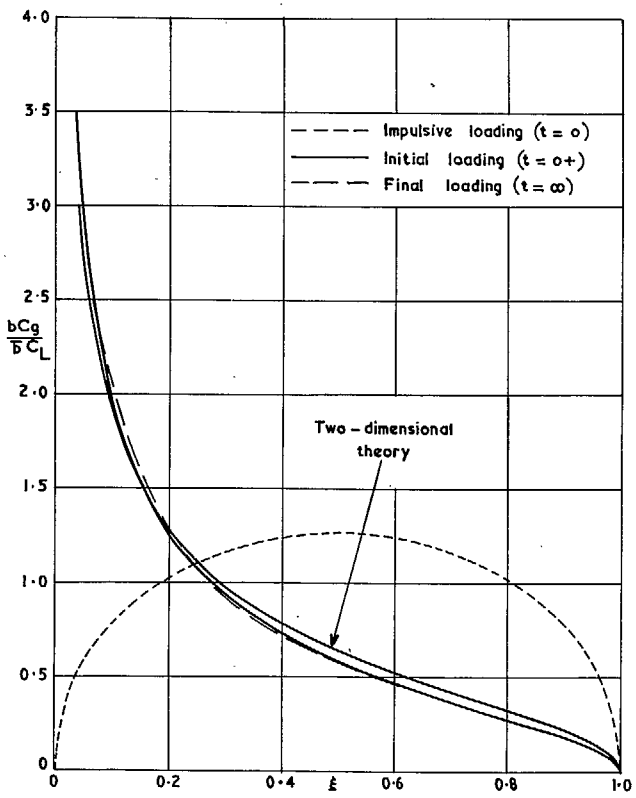

FIG. 8. Initial and final chordwise loading on a rectangular wing ($A = 4$)

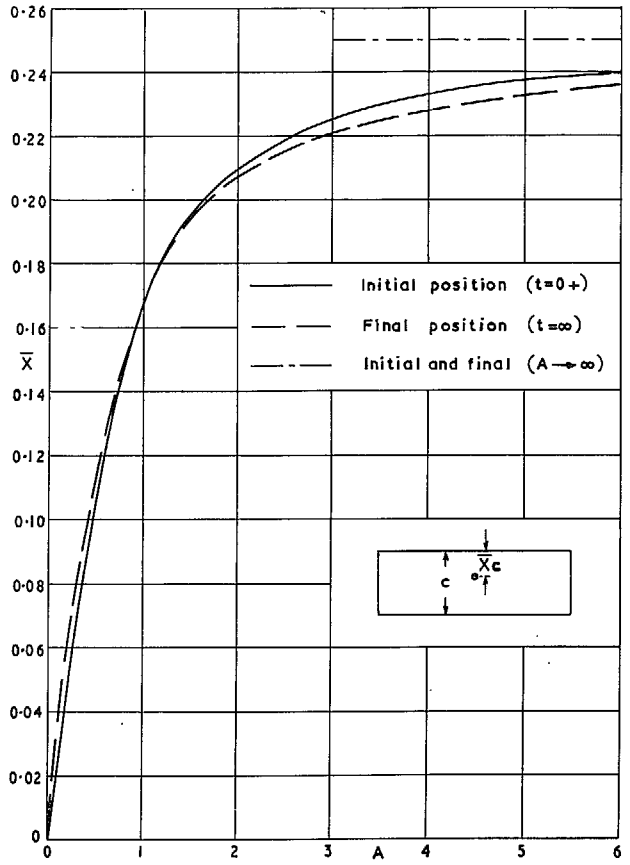

FIG. 9. Initial and final centres of lift for rectangular wings

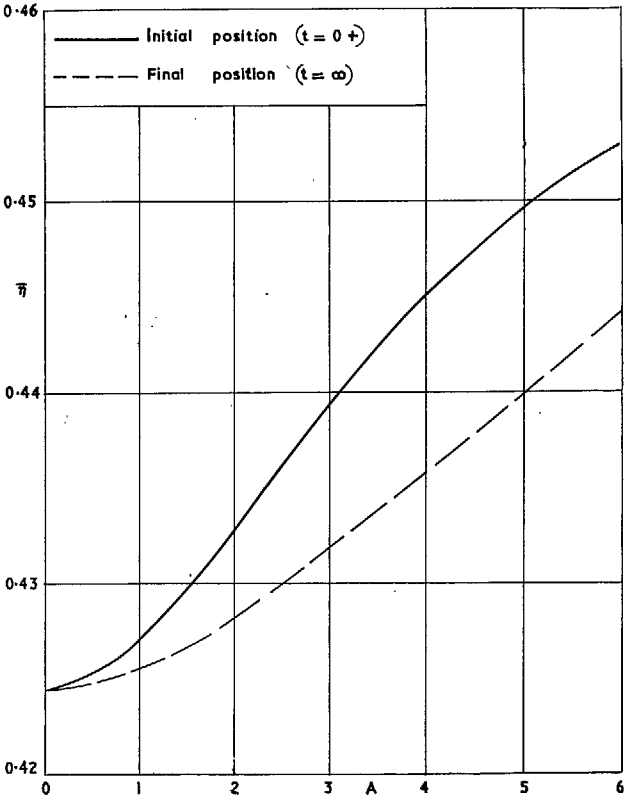

FIG. 10. Initial and final spanwise centres of lift for rectangular wings

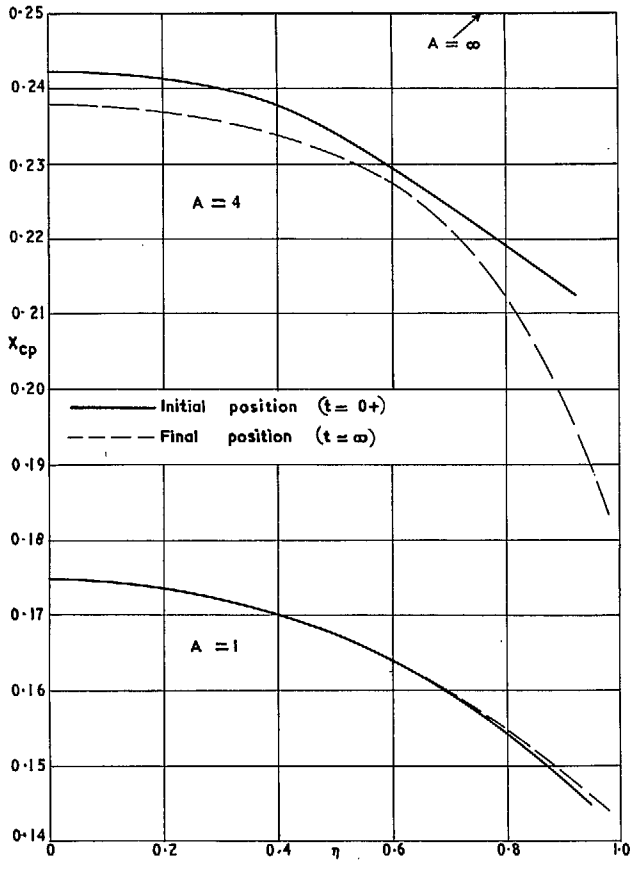

FIG. 11. Initial and final spanwise distributions of centre of pressure for rectangular wings

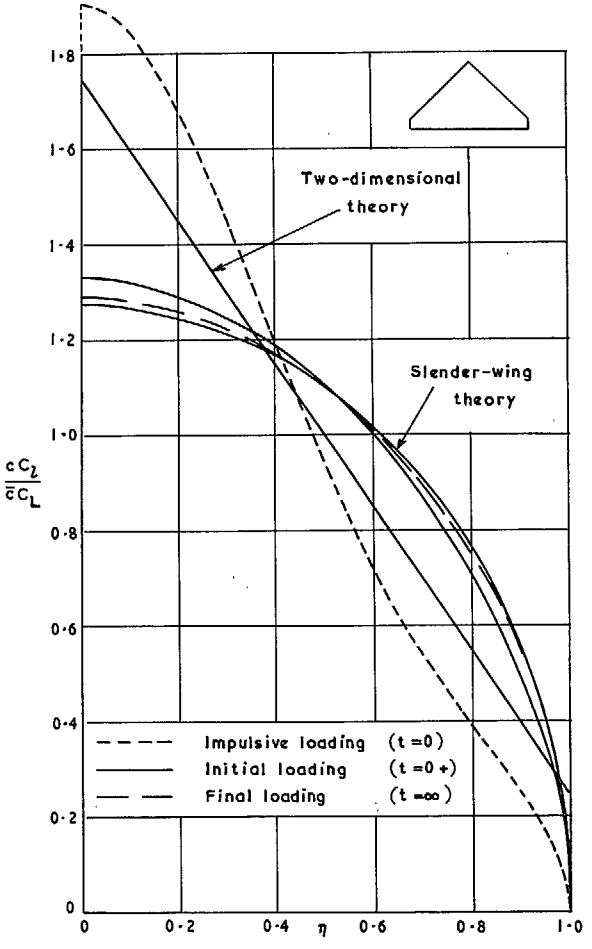

FIG. 12. Initial and final spanwise loading on a delta wing ($A = 3$, $\lambda = 1/7$)

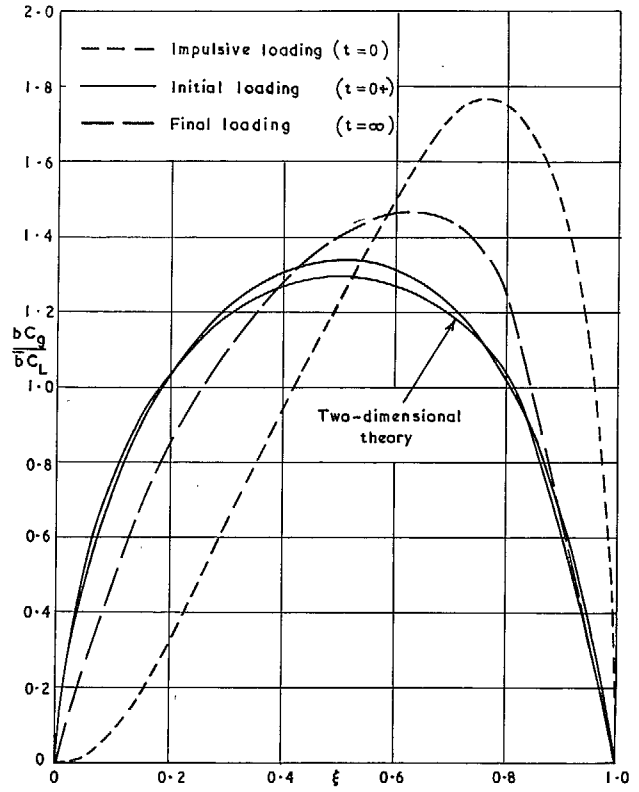

Fig.13. Initial and final chordwise loading on a delta wing ($A = 3, \lambda = 1/7$)

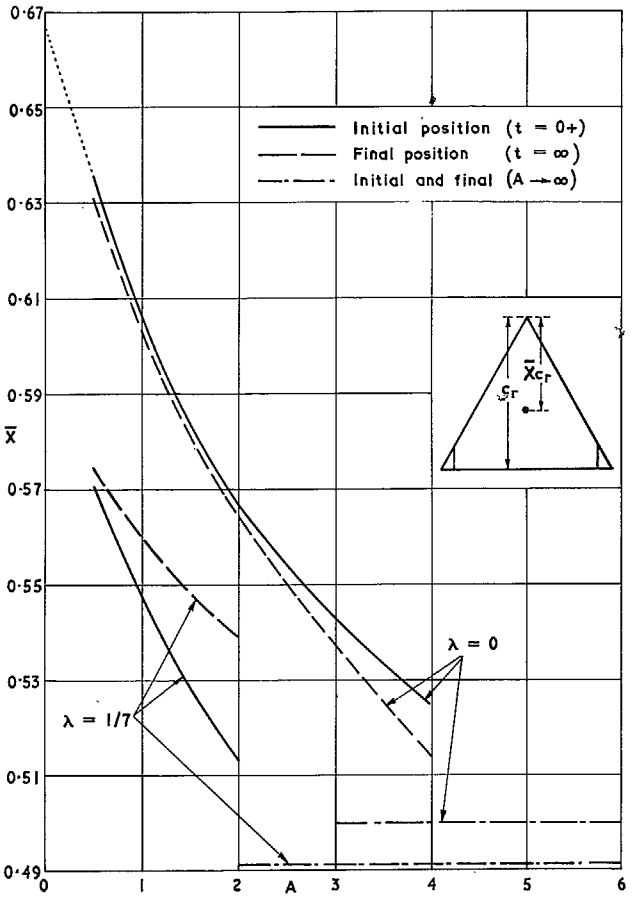

FIG. 14. Initial and final centres of lift for delta wings

Part II.—Transient Lift and Moment Functions for Rectangular and Delta Wings

Summary.

Transient lift and moment functions are considered for the cases of

(i) a sudden plunging motion,

(ii) entry into a sharp-edged gust.

Linearized theory is used and incompressibility of the fluid is assumed.

For sudden plunging motion, the functions are calculated from the lift and pitching moment coefficients associated with wings in oscillatory plunging motion. Results are presented for rectangular and complete delta wings of aspect ratios 1, 2 and 4.

Growth of lift functions due to gust entry are also calculated for these wings from knowledge of the corresponding functions due to sudden plunging motion. The method of analysis involves an application of a reverse flow theorem and an approximate relationship for the transient chordwise load distribution due to sudden plunging motion. It is uncertain whether the growth of pitching moment due to gust entry could be obtained accurately enough by a similar method. An alternative method is used to confirm the accuracy of the growth of lift function due to gust entry for a square wing. Calculations of this function by a simpler method for rectangular wings of high aspect ratio show reasonable agreement with those for aspect ratio 4; in addition, the exact solution for delta wings is derived for the limiting case of infinite aspect ratio.

LIST OF CONTENTS

Section

1. Introduction

2. Wings in Sudden Plunging Motion

   2.1 Approximate method of solution

   2.2 Results for rectangular and delta wings

3. Wings Entering Sharp-Edged Gusts

   3.1 Method of solution for rectangular wings

   3.2 Alternative solution for rectangular wings

   3.3 Solution for delta wings

   3.4 Limitations on applicability of method

4. Gust Entry for Wings of High Aspect Ratio

5. Acknowledgement

List of Symbols

References

Tables 1 to 3

1. *Introduction.*

The lift functions due to sudden plunging motion and to entry into a sharp-edged gust are of fundamental importance for the calculation of lift forces due to more general transient motions. For two-dimensional wings, the original derivation of these respective functions is universally attributed to Wagner[1] and Küssner[2].

Several writers have given approximate solutions for the growth of lift function, $k_1(s)$, for finite wings in sudden plunging motion. However, there appears to be very little information in the literature as regards the corresponding moment function, $m_1(s)$. In the present report both functions are calculated for rectangular and complete delta wings of aspect ratios 1, 2 and 4. The functions are expressed in terms of the lift and moment coefficients associated with oscillatory plunging motion by means of the reciprocal relations given by Garrick[3]. Values of the oscillatory coefficients for finite frequencies are taken from the theoretical work of Lawrence and Gerber[4], whilst the values corresponding to infinite frequency are deduced from Part 1 of this report.

Assuming a knowledge of $k_1(s)$, we suggest a simple method for calculating the growth of lift function, $k_2(s)$, for finite wings on entry into a stationary, sharp-edged gust. As a consequence, the lift force may be calculated on finite wings entering sharp-edged gusts which travel in the streamwise direction. Such calculations have been made for two-dimensional wings by Drischler and Diederich[5],

On the basis of these methods, formulae for $k_2(s)$ can be derived for wings of high aspect ratio and of not too extreme planform. Such formulae are given here for rectangular and delta wings; the result for a rectangular wing entering a stationary gust is identical with that of W. P. Jones[6].

Mention should be made of the neglect of compressibility in the present work. The subsonic, compressible solution for sudden plunging motion is non-uniform at $t = 0$ in the limit as Mach number tends to zero. However, the practical problem is concerned, not with sudden plunging motion, but with latter motions can be evaluated from $k_1(s)$ by the principle of superposition and are not expected to depend critically on Mach number below the transonic range. For sharp-edged gusts the function $k_2(s)$ is independent uf Mach number for slender wings.

2. *Wings in Sudden Plunging Motion.*

We consider the motion of a thin, flat wing moving with constant velocity U and at zero incidence for time $t<0$. At $t = 0$ the wing starts to plunge with uniform velocity $U\alpha$. The non-dimensional distance travelled is defined as

$$s = 2\frac{Ut}{c},$$

where c is the streamwise extent of the planform. Under the assumption of linearized theory, the growth of lift function for this sudden plunging motion can be calculated from either the real or the imaginary part of the complex lift coefficient for oscillatory plunging motion (*see*, for example, Garrick[3]).

Thus, for $s>0$,

$$C_L(s) = \frac{L_1(s)}{\frac{1}{2}\rho U^2 S} = \frac{2\alpha}{\pi}\int_0^\infty \frac{F(v)\sin vs}{v}dv \tag{1}$$

or

$$C_L(s) = \alpha\left[1+\frac{2}{\pi}\int_0^\infty \frac{G(v)\cos vs}{v}dv\right], \tag{2}$$

where the oscillatory lift coefficient is the real part of

$$iv[F(v)+iG(v)]e^{ivs}$$

for a reduced frequency of oscillation

$$\nu = \frac{\omega c}{2U}.$$

Unfortunately, the analytical forms of $F(\nu)$ and $G(\nu)$ are not known. In the remainder of this section we shall only make use of equation (1), since it is more convenient for numerical work than equation (2).

2.1. *Approximate Method of Solution.*
We first write

$$F(\nu) = F(0) + \sum_{r=1}^{n} \frac{a_r \nu^2}{b_r^2 + \nu^2}, \tag{3}$$

where the constants a_r and b_r would be found from known numerical values of $F(\nu)$. On substituting equation (3) into equation (1) we obtain

$$C_L(s) = \alpha \left[F(0) + \sum_{r=1}^{n} a_r e^{-|b_r|s} \right]. \tag{4}$$

It is found that $C_L(s)$ can be represented with sufficient accuracy by taking $n = 1$ for wings of aspect ratio $A = 1$, 2 and 4 (*see* also Ref. 6). The constant a_1 is then given by

$$a_1 = F(\infty) - F(0), \tag{5}$$

and b_1 chosen to give the best approximation to $F(\nu)$. The effect of this procedure is illustrated in Fig. 1. Then

$$k_1(s) = \frac{C_L(s)}{C_L(\infty)} = 1 - \frac{F(0) - F(\infty)}{F(0)} e^{-|b_1|s}. \tag{6}$$

The pitching moment due to sudden plunging motion can be calculated in the same way. For $s > 0$,

$$C_m(s) = \frac{M_1(s)}{\frac{1}{2}\rho U^2 Sc} = \frac{2\alpha}{\pi} \int_0^\infty \frac{M(\nu) \sin \nu s}{\nu} d\nu \tag{7}$$

or

$$C_m(s) = \alpha \left[1 + \frac{2}{\pi} \int_0^\infty \frac{N(\nu) \cos \nu s}{\nu} d\nu \right], \tag{8}$$

where the oscillatory pitching moment coefficient is the real part of

$$i\nu [M(\nu) + iN(\nu)] e^{i\nu s}.$$

On writing

$$M(\nu) = M(0) + \sum_{r=1}^{n} \frac{p_r \nu^2}{q_r^2 + \nu^2} \tag{9}$$

and substituting into equation (7), we find

$$C_m(s) = \alpha\left[M(0)+\sum_{r=1}^{n} p_r e^{-|q_r|s}\right]. \tag{10}$$

In particular, with $n = 1$,

$$m_1(s) = \frac{C_m(s)}{C_m(\infty)} = 1-\frac{M(0)-M(\infty)}{M(0)}e^{-|q_1|s}. \tag{11}$$

It can be shown from equations (1) and (7) that in the limits as $s\to\infty$ and $s\to 0+$

$$C_L(\infty) = \alpha F(0), \qquad C_m(\infty) = \alpha M(0), \tag{12}$$

and

$$C_L(0+) = \alpha F(\infty), \quad C_m(0+) = \alpha M(\infty). \tag{13}$$

The result in equation (13) has been shown, for example, by Mazelsky[7].

2.2. *Results for Rectangular and Delta Wings.*

Growth of lift and moment functions, $k_1(s)$ and $m_1(s)$, have been calculated by the method of Section 2.1 for rectangular and complete delta wings of aspect ratios 1, 2 and 4. The numerical information concerning $F(v)$ and $M(v)$ was obtained as follows:

(a) In accordance with equation (12) the steady-state values corresponding to $v = 0$ were taken from Ref. 8.

(b) Values for finite, non-zero v were taken from Ref. 4.

(c) In accordance with equation (13) values for $v = \infty$ were taken from the low-aspect-ratio method given in Part I.

All three methods are based on the same approximation so that, in this respect, the calculations for the functions $F(v)$ and $M(v)$ are consistent. The functions corresponding to equations (6) and (11) are given in Table 1. Curves of $k_1(s)$ are shown in Fig. 2 for rectangular wings of aspect ratios $A = 0, 1, 2, 4$ and ∞*. Corresponding curves for delta wings are shown in Fig. 3 with some incomplete results of Drischler[9] for comparison. The position of the centre of lift referred to the leading edge or apex,

$$\left.\begin{aligned} \bar{X}(s) &= \tfrac{1}{2}-\frac{C_m(s)}{C_L(s)} \quad \text{(rectangular wings)} \\ \bar{X}(s) &= -\frac{C_m(s)}{C_L(s)} \quad \text{(delta wings)} \end{aligned}\right\}, \tag{14}$$

is shown in Figs. 4 and 5 for $A = 1, 2, 4$ and ∞, while for $A = 0$, $\bar{X}(s) \equiv \bar{X}(\infty)$. Of particular note is the insignificant variation in $\bar{X}$ with s for all the rectangular wings.

---

*The curve corresponding to $A = \infty$ has been taken from equation (53) of Ref. 6.

3. *Wings Entering Sharp-Edged Gusts.*

By using the principle of superposition and following Drischler and Diederich[5], we can write the lift function for wings entering stationary, sharp-edged gusts as

$$L_2(s) = -\int_0^{\min(s,2)} \left[\frac{\partial}{\partial s_f} L_1(s-\sigma, s_f)\right]_{s_f=\sigma} d\sigma. \tag{15}$$

In this equation, $L_1(s,s_f)$ is the lift function for a rigid, hinged plate suddenly starting from rest with uniform forward velocity U and with local incidence

$$\left.\begin{aligned} \alpha(x) &= 0 \text{ for } o \leqslant x \leqslant \tfrac{1}{2}cs_f \\ \alpha(x) &= \alpha \text{ for } c \geqslant x > \tfrac{1}{2}cs_f \end{aligned}\right\}. \tag{16}$$

It should be noted that L_1 must be defined so as to include the effects of apparent mass.

One way of using equation (15) would be to find $L_1(s,s_f)$ from knowledge of the lift due to harmonically plunging flaps, by an analysis similar to that in Section 2. Although possible in principle, this method would be rather tedious and would demand knowledge of the oscillatory lift coefficients for a wide range of both v and flap-chord ratio. Fortunately, we can adopt another approach and find $L_1(s,s_f)$ by using a reverse flow theorem for indicial motion given by Heaslet and Spreiter[10]. In fact, on applying equation (45) of Ref. 10,

$$L_1(s,s_f) = \int_0^{c(1-\frac{1}{2}s_f)} g_1(\tilde{x},s)d\tilde{x} + \frac{\delta(s)}{\frac{1}{2}c}\int_0^{c(1-\frac{1}{2}s_f)} h(\tilde{x})d\tilde{x}, \tag{17}$$

where $\tilde{x}$ denotes the streamwise co-ordinate for the flat wing in reverse flight and $\delta(s)$ is the Dirac delta function defined by

$$\left.\begin{aligned} \delta(s) &= 0 \text{ for } s \neq 0 \\ \delta(s) &= \infty \text{ for } s = 0 \\ \int_{-\infty}^{\infty} \delta(s)ds &= 1 \end{aligned}\right\}. \tag{18}$$

The quantity $g_1(\tilde{x},s)$ is the spanwise integral of loading following the sudden plunging motion of the flat wing in reverse flight. The function $h'(\tilde{x}) = dh/d\tilde{x}$ represents the same integral for the flat wing in steady, reverse flight in the absence of circulation. Little is known about the function g_1 for finite wings, but $h(\tilde{x})$ can be determined and has been calculated in Part I for rectangular and delta wings of many aspect ratios.

3.1. *Method of Solution for Rectangular Wings.*

For rectangular wings x and $\tilde{x}$ are interchangeable and we shall assume that

$$g_1(\tilde{x},s) = g_1(x,s) = k_1(s)g_1(x,\infty), \tag{19}$$

for the particular aspect ratios 1, 2 and 4. This amounts to neglecting effects of any variation in chordwise load distribution, $cg_1(x,s)/L_1(s)$, for $s>0$. The available evidence strongly suggests that introduction of equation (19) should not lead to any serious error:

(a) During the sudden plunging motion ($s>0$), the variation in position of centre of lift is insignificant (Fig. 4).

(b) As discussed in Part I, the differences in the initial ($s = 0+$) and final ($s = \infty$) chordwise load distributions are insignificant (Fig. 6).

(c) The differences in initial and final spanwise load distributions are significant at $A = 1, 2$ and small at $A = 4$ (Part I); moreover, the spanwise distribution moves gradually from its initial to its final distribution (Refs. 9 and 11).

In addition, we point out that equation (19) holds exactly for $A = 0$ and $A = \infty$.

Combined use of equations (15) to (19) gives

$$k_2(s)L_2(\infty) = L_2(s) = \tfrac{1}{2}c \int_0^s k_1(s-\sigma)g_1(c-\tfrac{1}{2}c\sigma,\infty)d\sigma + h(c-\tfrac{1}{2}cs), \tag{20}$$

when $s \leqslant 2$. For $s > 2$, the upper limit of the integral is placed by 2 and the second term vanishes. The approximation of equation (19) has been used only in the integral.

The steady-state chordwise loading, $g_1(x,\infty)$ has been calculated by Goodman[8] whilst $h(x)$ can be found from Part I. In fact,

$$g_1(x,\infty) = 2\rho U^2\alpha\left(\frac{b^2}{c}\right)\left(A_0\tan\tfrac{1}{2}\psi + 2\sum_{r=1}^{5} A_r \sin r\psi\right), \tag{21}$$

$$\left.\begin{aligned} h(x) &= \frac{1}{4}\pi\rho U^2\alpha b^2 \sum_{r=1}^{4} D_{2r-1}\frac{\sin(2r-1)\psi}{2r-1} \\ &= \frac{1}{4}\pi\rho U^2\alpha b^2 \sum_{r=1}^{4} \overline{D}_{2r-1}\sin^{2r-1}\psi \end{aligned}\right\} \tag{22}$$

where $2x = c(1+\cos\psi)$. We write the definite series of equation (21) in terms of $\sin^r\psi$ (r odd) and $\cos\psi\sin^{r-1}\psi$ (r even). With these substitutions equation (20) may be written as

$$C_L(\infty)k_2(s) = 2A\alpha \int_0^s k_1(s-\sigma)\left\{\bar{A}_0\left[\frac{\sigma}{2-\sigma}\right]^{\frac{1}{2}} + \sum_{r=1}^{3}\left[\bar{A}_{2r-1} + (1-\sigma)\bar{A}_{2r}\right]\left[\sigma(2-\sigma)\right]^{\frac{2r-1}{2}}\right\} d\sigma +$$

$$+\frac{1}{2}\pi A\alpha \sum_{r=1}^{4} \overline{D}_{2r-1}\left[s(2-s)\right]^{\frac{2r-1}{2}}, \quad (0 \leqslant s \leqslant 2), \tag{23}$$

where $\bar{A}_0 = A_0$ and $\bar{A}_6 = 0$. For $s > 2$, the upper limit of the integral is replaced by 2 and the second term vanishes. The lift coefficient for steady flow is given by

$$C_L(\infty) = 2\pi A(A_0 + A_1)\alpha. \tag{24}$$

The constants A_r, $\bar{A}_r$ are given in Table 2 whilst the quantities D_{2r-1} can be found in Part I. Values of $k_2(s)$ as calculated from equation (23) are given in Table 3(a) for rectangular wings $A = 1, 2$ and 4. Corresponding curves are shown in Fig. 7 together with a curve for $A = \infty$ plotted from Table 1 of Ref. 6.

3.2. *Alternative Solution for Rectangular Wings.*

It is pointed out that there is a very slight discrepancy in equation (23) leading to a singularity at $s = 2$. Although $k_2(s)$ in equation (23) is continuous at $s = 2$, its derivatives are not. In fact, when $0 \leqslant s \leqslant 2$, $k_2'(s)$ contains two terms in $(2-s)^{-1/2}$. These terms cancel identically at $s = 2$ when $A = \infty$, but this is only approximately true in the method given in Section 3.1. However, the resulting discrepancy is very small and cannot be detected in Fig. 7.

It follows from the exact form of equation (20) that the derivative $L_2'(s)$ is continuous at $s = 2$ provided

$$g_1(o,0+)-h'(o) = 0;$$

this in fact holds as can easily be deduced from equation (A1) of Part I. Thus, we adopt an alternative approach to avoid the spurious discontinuity at $s = 2$. For, instead of equation (19), we may write

$$g_1(x,s) = \frac{k_1(s)}{k_1(0+)} g_1(x,0+). \tag{25}$$

In Part I, the initial chordwise loading is given for rectangular wings as

$$g_1(x,0+) = -\frac{1}{4}\pi\rho U^2 A\alpha b \left[\tan\tfrac{1}{2}\psi \sum_{r=1}^{4} D_{2r-1}\cos(2r-1)\psi + A\sum_{r=1}^{4} D'_{2r-1}\frac{\sin(2r-1)\psi}{2r-1}\right], \tag{26}$$

where $D'_{2r-1} = dD_{2r-1}/dA$. When this expression is substituted into equation (20), we obtain

$$C_L(\infty)k_2(s) = -\frac{1}{4}\pi A\alpha \int_0^s \frac{k_1(s-\sigma)}{k_1(0+)} \left[\tan\tfrac{1}{2}\psi \sum_{r=1}^{4} D_{2r-1}\cos(2r-1)\psi + A\sum_{r=1}^{4} D'_{2r-1}\frac{\sin(2r-1)\psi}{2r-1}\right]_{\cos\psi = 1-\sigma} d\sigma +$$

$$+\frac{1}{2}\pi A\alpha \left[\sum_{r=1}^{4} D_{2r-1}\frac{\sin(2r-1)\psi'}{2r-1}\right]_{\cos\psi' = 1-s}, \tag{27}$$

where $0 \leqslant s \leqslant 2$. It naturally follows from equation (27) that $k_2'(s)$ is now continuous at $s = 2$, the contribution from the two terms in $(2-s)^{-\frac{1}{2}}$ vanishing at $s = 2$.

Use of the method of Section 3.1 for the rectangular wings $A = 1, 2$ and 4 shows that

$$\lim_{s\to 2} (2-s)^{\frac{1}{2}} k_2'(s)$$

is greatest when $A = 1$. Hence, for this aspect ratio, $k_2(s)$ was also calculated by the alternative method as given in equation (27). The difference in the two calculations of $k_2(s)$ was less than 0·0002 near $s = 2$ and nowhere exceeded 0·0014.

3.3. *Solution for Delta Wings.*

The methods of calculation described for rectangular wings in Sections 3.1 and 2.2 are both applicable to delta wings. However, whilst the method of calculating $g_1(\tilde{x},\infty)$ described in Ref. 8 is not valid for delta wings in reverse flight, there is no restriction in the method of Part I for $g_1(\tilde{x},0+)$. Thus, for the complete delta wings considered here, we use the alternative method of Section 3.2. The supporting evidence is as follows:

(a) During the sudden plunging motion, the variation in position of centre of lift is insignificant for a complete delta wing ($A = 2$) in reverse flight; in fact $0{\cdot}0990 \leqslant \overline{X}(s) \leqslant 0{\cdot}0999$ for all s.

(b) The differences in the initial ($s = 0+$) and final ($s = \infty$) chordwise load distributions are insignificant for a cropped delta wing† ($A = 1{\cdot}8$) of taper ratio 1/7.

In addition, equation (25) for delta wings in reverse flight holds exactly when $A = 0$ and $A = \infty$.

Values of $k_2(s)$ are given in Table 3(b) for aspect ratios $A = 1$, 2 and 4 together with values for $A = 0$ from slender-wing theory. The corresponding curves are reproduced in Fig. 8.

3.4. *Limitations on Applicability of Method.*

No mention has so far been made of the pitching moment function, $m_2(s)$, due to gust entry. There exists a relationship, identical in form to equation (15), connecting the corresponding pitching moment $M_2(s)$ and that due to the indicial motion from rest of the rigid, hinged plate of equation (16). The pitching moment of the hinged plate about an arbitrary axis $x = c\xi$ can be related, by means of the reverse flow theorems of Ref. 10, to the streamwise integral of lift due to indicial motion of a cambered wing with downwash distribution proportional to $c(1-\xi)-\tilde{x}$. For simplicity we should, if possible, choose ξ so that the chordwise load distribution is unchanged throughout the indicial motion $s>0$. In the case of two-dimensional wings the procedure is clear. According to Lomax[12], the only downwash distribution depending linearly on $\tilde{x}$ and producing a lift distribution which never varies for $s>0$ is found by taking $\xi = \frac{1}{4}$; this implies that the total indicial lift on the cambered wing is identically zero. By making use of the lift distribution in the case $\xi = \frac{1}{4}$, it can be shown without difficulty that

$$[M_2(s)]_{\frac{1}{4}-\text{chord}} \equiv 0,$$

as first predicted by Küssner[2]. In the case of finite rectangular wings we might suppose that the corresponding procedure would be to consider a pitching axis $x = c\overline{X}(A,s) \approx c\overline{X}(A)$ as given in Fig. 4. Unfortunately, it is not known whether the chordwise load distribution for a downwash proportional to $c[1-\overline{X}(A)]-\tilde{x}$ is unchanged throughout the indicial motion $s>0$; even the distribution at $s = 0+$ is not, at present, known. Hence, we cannot justify a general approximation similar to equation (19), and so no calculations of $m_2(s)$ have been attempted. Nevertheless, for fairly slender wings, such an approximation might well be made with success, since the limiting chordwise distribution on the cambered wing ($A\to 0$) is unchanged throughout the indicial motion $s>0$: then evaluation of the expression corresponding to equation (20) should give a distinct improvement on slender-wing theory.

4. *Gust Entry for Wings of High Aspect Ratio.*

We shall again use equations (15) to (18) together with the assumption of equation (19),

$$g_1(\tilde{x},s) = k_1(s)g_1(\tilde{x},\infty).$$

For wings of high aspect ratio and of not too extreme planform $g_1(\tilde{x},\infty)$ and $h(\tilde{x})$ may be found by two-dimensional strip theory for the wing in reverse flight. Thus,

---

†The final, steady-state loading $g_1(\tilde{x},\infty)$ was not available for the complete delta wing ($A = 2$) in reverse flight.

$$g_1(\tilde{x},\infty) = 2\rho U^2\alpha \left[\frac{C_L(\infty)}{2\pi\alpha}\right] \int_{-\frac{1}{2}b(\tilde{x})}^{\frac{1}{2}b(\tilde{x})} \left[\frac{\tilde{x}_1(y)-\tilde{x}}{\tilde{x}-\tilde{x}_0(y)}\right]^{\frac{1}{2}} dy, \tag{28}$$

where $\tilde{x} = \tilde{x}_0(y)$, $\tilde{x} = \tilde{x}_1(y)$ are the equations of the leading and trailing edges for the wing in reverse flight, and $b(\tilde{x})$ is the local span. Similarly,

$$h(\tilde{x}) = \frac{2\rho U^2\alpha C_N}{[C_N]_{A\to\infty}} \int_{-\frac{1}{2}b(\tilde{x})}^{\frac{1}{2}b(\tilde{x})} [\tilde{x}_1(y)-\tilde{x}]^{\frac{1}{2}} [\tilde{x}-\tilde{x}_0(y)]^{\frac{1}{2}} dy, \tag{29}$$

where C_N is the pitching moment coefficient for the wing in steady flow without circulation (Part I).

The method suggested above would apply, for example, to elliptic, rectangular and cropped delta wings, but not to wings of high sweep. If we now use the above formulae for $g_1(\tilde{x},\infty)$ and $h(\tilde{x})$ in equation (20), the following results are obtained:

(a) for rectangular wings of high aspect ratio,

$$\left.\begin{aligned} k_2(s) &= \frac{1}{\pi}\int_0^s k_1(s-\sigma)\left[\frac{\sigma}{2-\sigma}\right]^{\frac{1}{2}} d\sigma + \frac{4C_N}{\pi C_L(\infty)}[s(2-s)]^{\frac{1}{2}}, \quad (0\leqslant s\leqslant 2) \\ &= \frac{1}{\pi}\int_0^2 k_1(s-\sigma)\left[\frac{\sigma}{2-\sigma}\right]^{\frac{1}{2}} d\sigma, \quad (s>2) \end{aligned}\right\}. \tag{30}$$

Another derivation of these equations has been given by W. P. Jones[6].

(b) for complete delta wings of high aspect ratio,

$$\left.\begin{aligned} k_2(s) &= \frac{2}{3\pi}\int_0^s k_1(s-\sigma)\sigma\left[\frac{\sigma}{2-\sigma}\right]^{\frac{1}{2}} d\sigma + \frac{4C_N}{\pi C_L(\infty)} s[s(2-s)]^{\frac{1}{2}}, \quad (0\leqslant s\leqslant 2) \\ &= \frac{2}{3\pi}\int_0^2 k_1(s-\sigma)\sigma\left[\frac{\sigma}{2-\sigma}\right]^{\frac{1}{2}} d\sigma, \quad (s>2) \end{aligned}\right\}. \tag{31}$$

It is seen from equations (30) and (31) that $k_2(s)$ behaves near $s = 0$ like $s^{1/2}$ and $s^{3/2}$ for rectangular and delta wings respectively. A comparison is made in Fig. 9 between curves for the rectangular wing $A = 4$ plotted from W. P. Jones' calculations based on equation (30) and from the more accurate method of Section 3. The agreement is satisfactory. A curve from equation (31) for $A = \infty$ is included in Fig. 8. The asymptotic forms of $k_2(s)$ for large s are identical when $A\to\infty$, and it is seen from Figs. 7 and 8 that the differences are very small for $s\leqslant 2$; larger differences are found for the rectangular and delta wings of aspect ratio 4.

5. *Acknowledgement.*

The author gratefully acknowledges the assistance of Mrs. S. Lucas, who was responsible for the numerical calculations and who prepared the diagrams.

LIST OF SYMBOLS

A	Aspect ratio, b^2/S
A_r	Coefficients in equation (21)
b	Wing span
$b(x)$	Local span
c	Streamwise extent of planform
$C_L(s)$	Lift coefficient, lift/$(\frac{1}{2}\rho U^2 S)$
$C_m(s)$	Pitching moment coefficient, $M_1(s)/(\frac{1}{2}\rho U^2 Sc)$
C_N	Pitching moment coefficient for steady flow without circulation
D_r	Coefficients in equation (22)
$F(v)$	Defined below equation (2)
$g_1(\tilde{x},s)$	Chordwise loading function for sudden plunging motion
$h(\tilde{x})$	Streamwise lift integral for steady reverse flow without circulation (Part I)
$k_1(s)$	Ratio of transient lift to final lift during sudden plunging motion
$k_2(s)$	Ratio of transient lift to final lift during gust entry
$L_1(s)$	Total lift on wing in sudden plunging motion
$L_2(s)$	Total lift on wing due to gust entry
$m_1(s)$	Ratio of transient pitching moment to final pitching moment during sudden plunging motion
$M(v)$	Defined below equation (8)
$M_1(s)$	Nose-up pitching moment in sudden plunging motion (about axis through mid-chord of rectangular wing or apex of delta wing)
s	Non-dimensional distance travelled, $2Ut/c$
s_f	Value of $2x/c$ at hinge position in equation (16)
S	Area of planform
t	Time, measured from sudden plunge or from entry into a gust
U	Flight velocity
x	Streamwise distance from the leading edge
$\tilde{x}$	Streamwise distance in reverse flow, (c−x)
$\overline{X}(s)$	Centre of lift in equation (14)
α	Incidence
$\delta(s)$	Dirac delta function in equation (18)
v	Reduced frequency of oscillation, $\omega c/2U$
ρ	Density
ψ	$\mathrm{Cos}^{-1}\left(\frac{2x}{c}-1\right)$
ω	Frequency of oscillation

REFERENCES

No.	*Author(s)*	*Title, etc.*
1	H. Wagner	Über die Entstehung des dynamischen Auftriebes von Tragflügeln. ZAMM, Bd. 5, February, 1925.
2	H. G. Küssner	Zusammenfassender Bericht über den instationären Auftrieb von Flügeln. Luftfahrtforschung, Bd. 13, December, 1936.
3	I. E. Garrick	On some reciprocal relations in the theory of non-stationary flows. N.A.C.A. Report 629, 1938.
4	H. R. Lawrence and E. H. Gerber	The aerodynamic forces on low-aspect-ratio wings oscillating in an incompressible flow. *J. Aero. Sci.*, Vol. 19, November, 1952.
5	J. A. Drischler and F. W. Diederich	Lift and moment responses to penetration of sharp-edged travelling gusts, with application to penetration of weak blast waves. N.A.C.A. Tech. Note 3956, May, 1957.
6	W. P. Jones	Aerodynamic forces on wings in non-uniform motion. A.R.C. R. and M. 2117, August, 1945.
7	B. Mazelsky	Numerical determination of indicial lift of a two-dimensional sinking airfoil at subsonic Mach numbers from oscillatory lift coefficients with calculations for Mach number 0·7. N.A.C.A. Tech. Note 2562, December, 1951.
8	Th. R. Goodman	Calculation of aerodynamic characteristics of low-aspect-ratio wings at subsonic speeds. Cornell Aero. Lab. Report, August, 1951.
9	J. A. Drischler	Approximate indicial lift functions for several wings of finite span in incompressible flow as obtained from oscillatory lift coefficients. N.A.C.A. Tech. Note 3639, May, 1956.
10	M. A. Heaslet and J. R. Spreiter	Reciprocity relations in aerodynamics. N.A.C.A. Report 1119, 1953.
11	U. Vogel	Ein Traglinienverfahren zur Berechnung der Auftriebsverteilung von Tragflügeln bei zeitabhängiger Vertikalbewegung. Z. Flugwiss, April, 1964.
12	H. Lomax	*Indicial Aerodynamics.* AGARD Manual on Aeroelasticity, Vol. II, Ch. 6.

TABLE 1

(a) *Functions for Rectangular Wings in Sudden Plunging Motion*

A	$k_1(s)$
1	$1-0{\cdot}069e^{-0{\cdot}750s}$
2	$1-0{\cdot}177e^{-0{\cdot}564s}$
4	$1-0{\cdot}299e^{-0{\cdot}405s}$

A	$m_1(s)$
1	$1-0{\cdot}068e^{-0{\cdot}730s}$
2	$1-0{\cdot}176e^{-0{\cdot}562s}$
4	$1-0{\cdot}298e^{-0{\cdot}404s}$

(b) *Functions for complete Delta Wings in Sudden Plunging Motion*

A	$k_1(s)$
1	$1-0{\cdot}071e^{-1{\cdot}569s}$
2	$1-0{\cdot}129e^{-0{\cdot}987s}$
4	$1-0{\cdot}203e^{-0{\cdot}903s}$

A	$m_1(s)$
1	$1-0{\cdot}066e^{-1{\cdot}917s}$
2	$1-0{\cdot}125e^{-1{\cdot}329s}$
4	$1-0{\cdot}186e^{-0{\cdot}903s}$

TABLE 2

Values of A_r and $\overline{A_r}$ for Rectangular Wings

(a) *Values of A_r*

A	A_0	A_1	A_2	A_3	A_4	A_5
1	0·3458	−0·1136	0·0369	−0·0111	0·0036	−0·0007
2	0·2418	−0·0454	0·0131	−0·0036	0·0012	−0·0003
4	0·1593	−0·0154	0·0044	−0·0011	0·0005	−0·0000

(b) *Values of $\overline{A_r}$*

A	$\overline{A_0}$	$\overline{A_1}$	$\overline{A_2}$	$\overline{A_3}$	$\overline{A_4}$	$\overline{A_5}$
1	0·3458	−0·3008	0·1764	0·1168	−0·0576	−0·0224
2	0·2418	−0·1154	0·0620	0·0408	−0·0192	−0·0096
4	0·1593	−0·0374	0·0216	0·0088	−0·0080	−0·0000

TABLE 3

(a) *Lift Function for Rectangular Wings Entering a Gust*

A	Values of $k_2(s)$ for $s =$						
	0·25	0·5	1·0	2·0	3·0	5·0	10·0
0	1·000	1·000	1·000	1·000	1·000	1·000	1·000
1	0·552	0·706	0·850	0·944	0·973	0·994	1·000
2	0·423	0·562	0·717	0·856	0·918	0·973	0·998
4	0·333	0·452	0·596	0·748	0·832	0·925	0·990
∞	0·223	0·306	0·417	0·551	0·635	0·739	0·856

(b) *Lift Function for Complete Delta Wings Entering a Gust*

A	Values of $k_2(s)$ for $s =$							
	0·25	0·5	1·0	1·5	2·0	3·0	5·0	10·0
0	0·016	0·063	0·250	0·563	1·000	1·000	1·000	1·000
1	0·014	0·073	0·306	0·644	0·946	0·989	0·999	1·000
2	0·020	0·094	0·345	0·652	0·894	0·960	0·994	1·000
4	0·035	0·126	0·372	0·631	0·823	0·898	0·966	0·998
∞	0·036	0·098	0·252	0·412	0·534	0·624	0·740	0·859

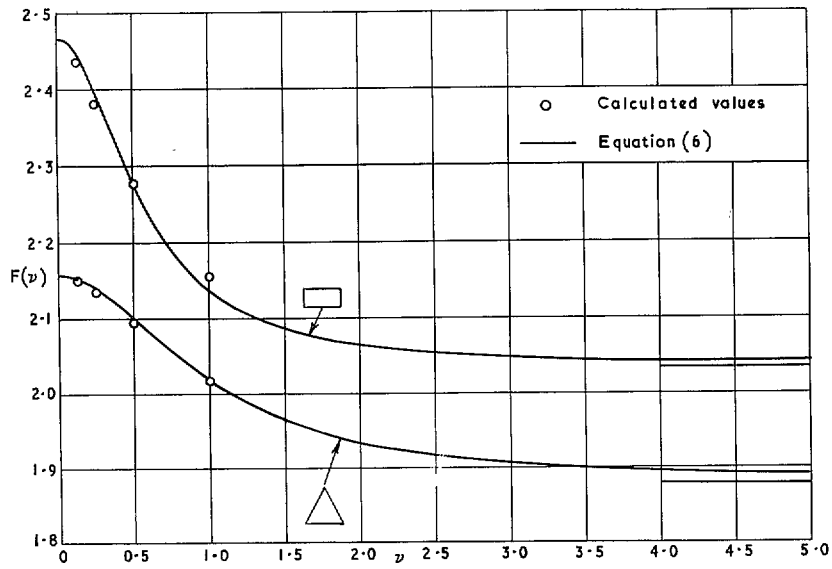

FIG. 1. Approximation to oscillatory lift function $F(\nu)$ for rectangular and delta wings of aspect ratio 2

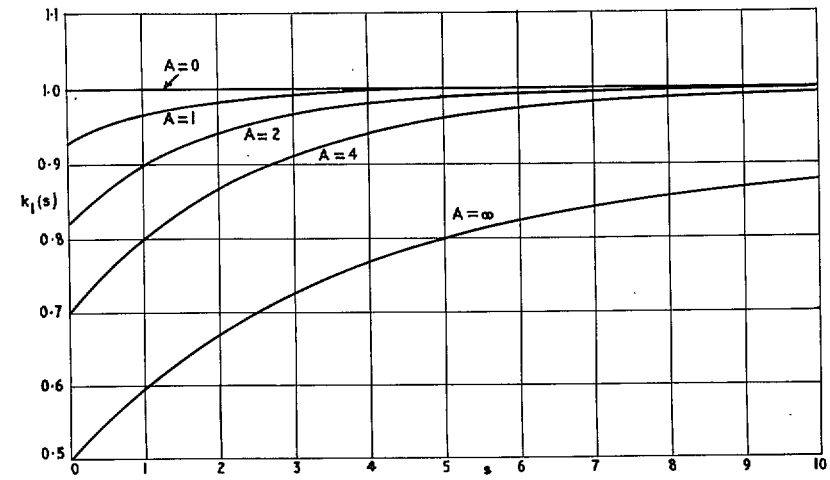

FIG. 2. Growth of lift for plunging rectangular wings of various aspect ratios

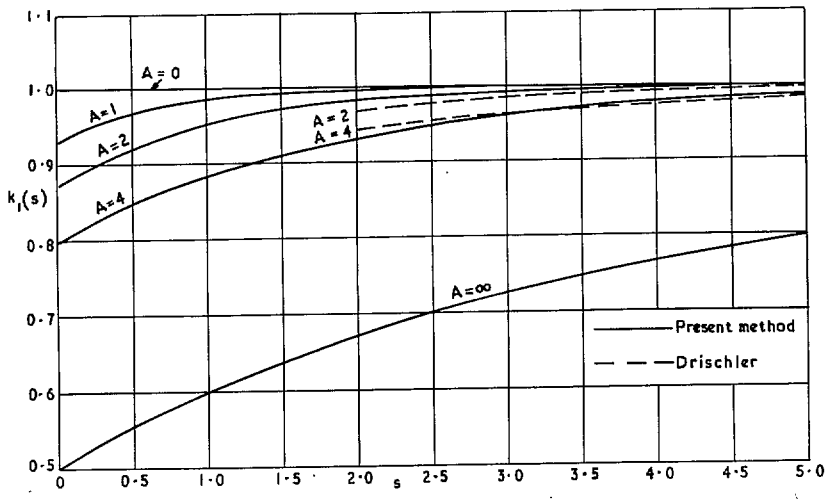

Growth of lift for plunging delta wings ($\lambda = 0$)

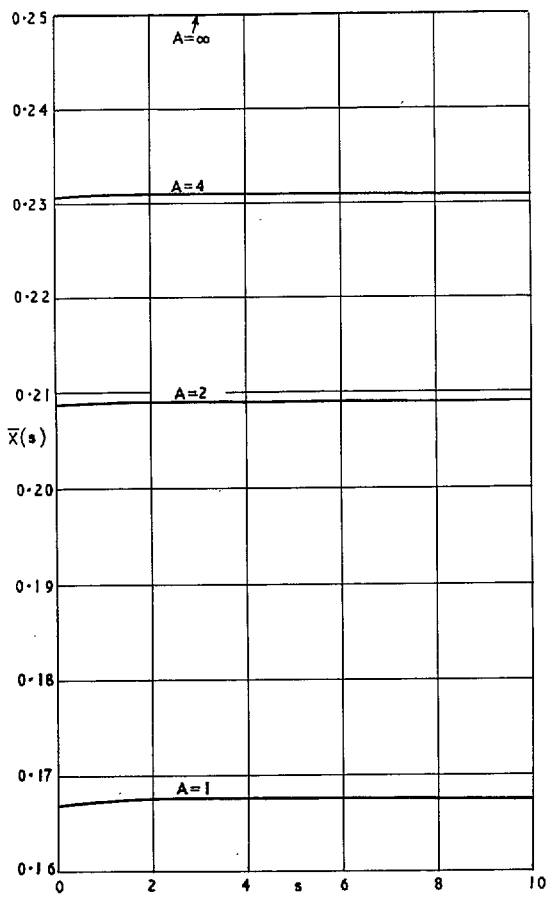

FIG. 4. Centre of lift on plunging rectangular wings

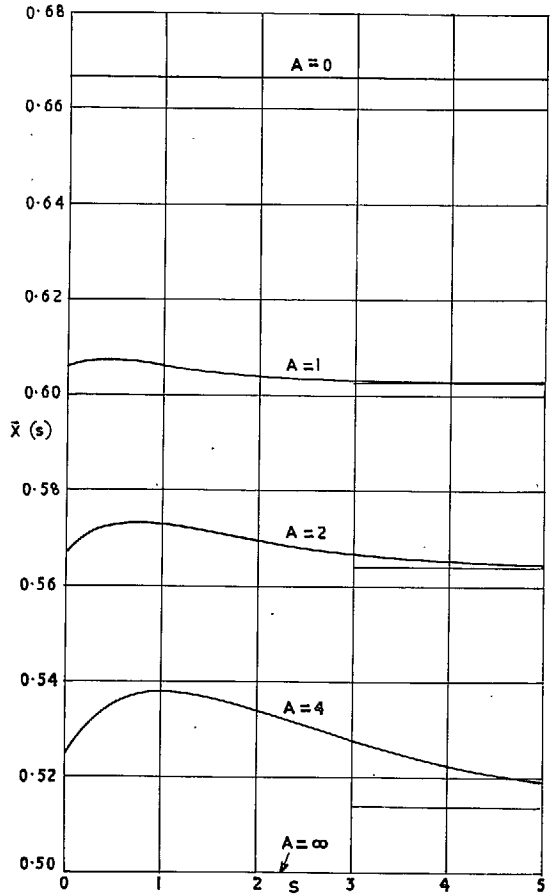

FIG. 5. Centre of lift on plunging delta wings ($\lambda = 0$)

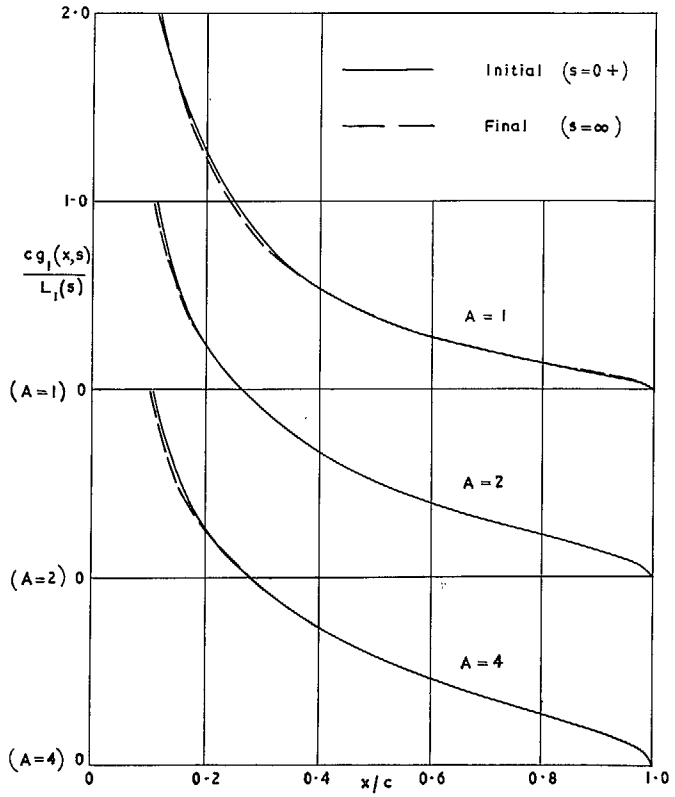

FIG. 6. Initial and final chordwise load distributions on plunging rectangular wings

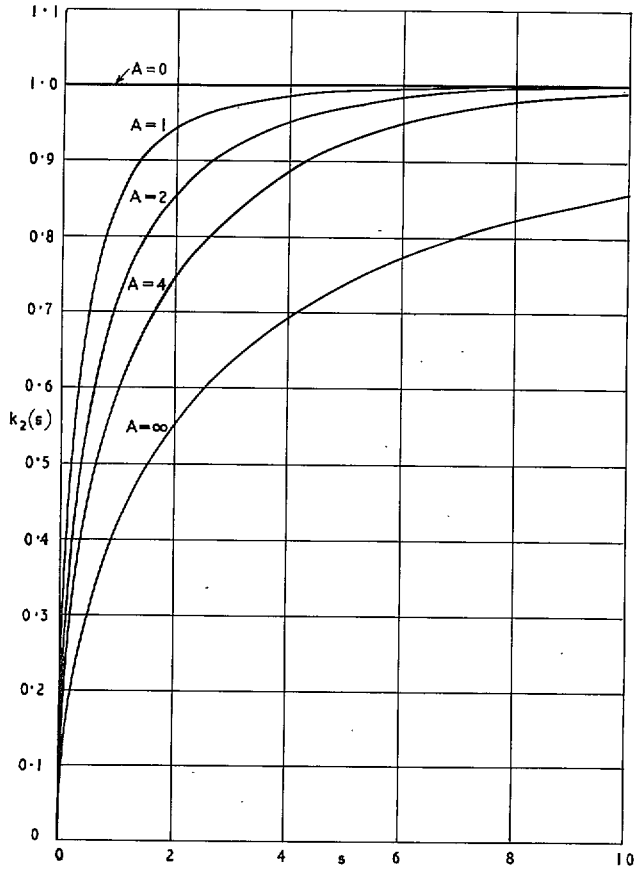

FIG. 7. Growth of lift for rectangular wings entering a sharp-edged gust

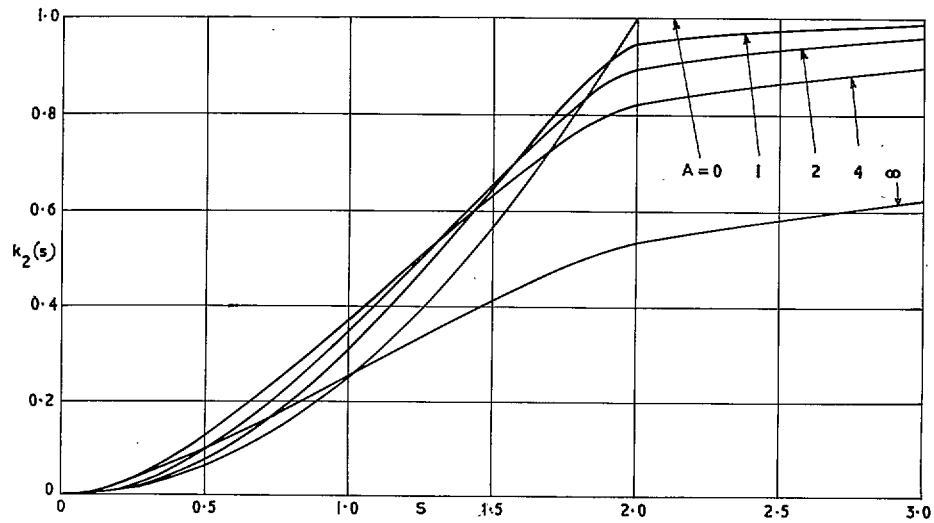

FIG. 8. Growth of lift delta wings ($\lambda = 0$) entering a sharp-edged gust

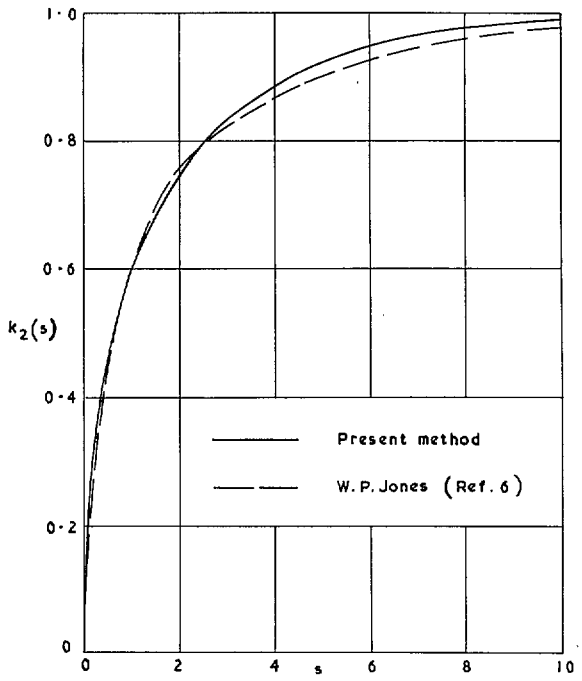

FIG. 9. Growth of lift on a rectangular wing ($A = 4$) entering a sharp-edged gust

Printed in Wales for Her Majesty's Stationery Office by Allens (Cardiff) Limited.

Dd.125874 K5 11/66

Published by
HER MAJESTY'S STATIONERY OFFICE

To be purchased from
49 High Holborn, London W.C.1
423 Oxford Street, London W.1
13A Castle Street, Edinburgh 2
109 St. Mary Street, Cardiff
Brazennose Street, Manchester 2
50 Fairfax Street, Bristol 1
35 Smallbrook, Ringway, Birmingham 5
80 Chichester Street, Belfast 1
or through any bookseller

S.O. Code No. 23–3456